Materials Horizons

ROYAL SOCIETY OF CHEMISTRY

REVIEW

View Article Online
View Journal | View Issue

Cite this: *Mater. Horiz.*, 2023, **10**, 3197

In situ stimulus-responsive self-assembled nanomaterials for drug delivery and disease treatment

Ziling Yan,†[a] Yanfei Liu,†[a] Licheng Zhao,[a] Jiaxin Hu,[b] Yimin Du,[b] Xingxing Peng[b] and Zhenbao Liu*[bc]

Received 19th April 2023,
Accepted 12th June 2023

DOI: 10.1039/d3mh00592e

rsc.li/materials-horizons

The individual motifs that respond to specific stimuli for the self-assembly of nanomaterials play important roles. *In situ* constructed nanomaterials are formed spontaneously without human intervention and have promising applications in bioscience. However, due to the complex physiological environment of the human body, designing stimulus-responsive self-assembled nanomaterials *in vivo* is a challenging problem for researchers. In this article, we discuss the self-assembly principles of various nanomaterials in response to the tissue microenvironment, cell membrane, and intracellular stimuli. We propose the applications and advantages of *in situ* self-assembly in drug delivery and disease diagnosis and treatment, with a focus on *in situ* self-assembly at the lesion site, especially in cancer. Additionally, we introduce the significance of introducing exogenous stimulation to construct self-assembly *in vivo*. Based on this foundation, we put forward the prospects and possible challenges in the field of *in situ* self-assembly. This review uncovers the relationship between the structure and properties of *in situ* self-assembled nanomaterials and provides new ideas for innovative drug molecular design and development to solve the problems in the targeted delivery and precision medicine.

Wider impact

In this review article, we discuss the relationship between the structure and properties of *in situ* self-assembled nanomaterials, with a focus on their potential for drug delivery, diagnosis and treatment of diseases. The driving forces behind the assembly of different chemical molecules are explored, enabling a deeper understanding of the *in vivo* microenvironment, cell surface, intracellular environment, and exogenous stimuli that promote self-assembly. As click chemistry and bioorthogonal chemistry continue to advance, chemical reactions that interfere with natural biochemical processes *in vivo* will become less of a concern, making *in situ* self-assembly an increasingly attractive approach for drug delivery and therapy. This review serves as a guideline for the design and development of future drug molecules, addressing targeted drug delivery and precision medicine from a new perspective.

1. Introduction

Nanomaterials, with a size ranging from 1–100 nm,[1] offer pharmacokinetic advantages such as longer blood circulation time,[2] membrane permeability,[3] and higher metabolic stability in the field of *in vivo* drug delivery.[4] They usually play a better role in adjuvant therapy. Although extensive research into nanomedicine in recent decades has led to many nanomaterial-based drug delivery strategies,[5] there is still a need to improve the morphology and residence time of drug-loaded nanoparticles (NPs) to enhance the delivery efficiency.[6] However, complex chemical reactions and physical interactions occur in organisms at any time, with an extraordinary ability to respond to external stimuli of different scales. In particular, the disease site is different from the microenvironment of normal tissues, such as the slightly acidic environment of tumor tissue, specific enzymes and receptors, the redox of tumor cells, and more.[7] Due to the complex physiological environment *in vivo*, nanodrug monomer molecules spontaneously assemble into larger aggregates due to changes in morphology and properties.[8] Generalized self-assembly is the process of basic structural units forming an

[a] *Department of Pharmaceutical Engineering, College of Chemistry and Chemical Engineering, Central South University, Changsha 410083, Hunan Province, P. R. China*
[b] *Department of Pharmaceutics, Xiangya School of Pharmaceutical Sciences, Central South University, Changsha 410013, Hunan Province, P. R. China. E-mail: zhenbaoliu@csu.edu.cn*
[c] *Molecular Imaging Research Center of Central South University, Changsha 410008, Hunan Province, P. R. China*
† These authors contributed equally to this work.

ordered structure in random disorder.[9] The concept of "*in vivo* self-assembly" was introduced in 2017.[10] *In vivo* self-assembled nanomedicines undergo blood circulation, tissue penetration, targeted accumulation, and elimination *in vitro*.[11] In contrast to *in vitro* self-assembled nanodrugs, *in situ* constructed self-assembled nanodrugs circulate in a molecular state, "self-assembly-assisted target" to the lesion site,[12] and accumulate in the pathological site through the aggregation/assembly-induced retention (AIR) effect,[13] which reduces the problems of rapid excretion and extensive metabolism, resulting in lower systemic toxicity.[14] Therefore, the *in situ* construction of stimuli-responsive self-assembled nanomaterials provides new ideas and strategies for diagnosing and treating major diseases such as cancer.

Self-assembly driving forces mainly include electrostatic interactions, hydrophobic interactions, hydrogen bonds,[15] and partial covalent bonding, such as the condensation reaction and cross-linking reaction in click chemical reactions, which may be a guide for optimizing the design of self-assembly.[16–18] Two electrolytes with opposite charges can form nanoscale assemblies on the surface of charged substrates by layer-by-layer adsorption due to electrostatic interactions.[19] Hydrogen bonds can be considered van der Waals forces between inherent dipoles. Hydrophobic interaction is a driving force that causes nonpolar substances to aggregate in aqueous solutions and repel water molecules. Hydrogen bonding and hydrophobic interaction complement each other and often co-exist in self-assembly.[20] In nonpolar solvents, hydrogen bonding is an important driving force for the association.[21] In particular, hydrogen bonding occurs not only in water but also in the interior of biological macromolecules, including the complementary pairing of the secondary structure of peptides and the double helix structure of deoxyribonucleic acid (DNA). In the α-helix of proteins, it is N–H···O-type hydrogen bonds, while in DNA molecules it is N–H···O and N–H···N-type hydrogen bonds.[22] In order not to be restricted by the natural synthesis *in vivo* and to covalently integrate biological signals into drugs and carriers, click chemical reactions are effective and cell-compatible and have been used to functionalize many self-assembly systems. This reaction makes new cellular microenvironment models have higher spatiotemporal complexity and flexibility than previously feasible.[23]

In the last two decades, a plethora of studies on molecular self-assembly have led to a deeper understanding of the basic principles and established the relationship between the structure and function of self-assembled systems. *In situ* self-assembly based on peptides has been widely discussed,[24–27] but this method is not limited to peptides, as other nanomaterials such as polymers,[28] small molecule prodrugs,[29] inorganic metals,[30] and nucleic acids[31,32] can also self-assemble. In this review, we discuss the principles of self-assembly of various nanomaterials in different microenvironments in the body, their applications, and the advantages of *in situ* self-assembly in drug delivery and disease diagnosis and treatment. We particularly focus on *in situ* self-assembly at lesion sites, especially in cancer. Additionally, we introduce the significance of introducing exogenous stimuli to construct self-assembly *in vivo*. Finally, we present perspectives and potential challenges in the field of *in situ* self-assembly. We hope that the *in situ* self-assembly strategy can provide novel ideas for drug molecular design and development to address targeted delivery and precision medicine challenges.

2. Self-assembly

2.1 Tissue microenvironment

Once absorbed by the body, drugs or drug delivery systems (DDS) are distributed through the blood circulation to various tissues and organs. The tissue microenvironment can be classified into two categories: normal and diseased tissue microenvironments. Among them, the tumor microenvironment plays a crucial role in tumor formation and development. Unlike normal tissues, the tumor tissue microenvironment contains various tumor-specific enzymes in the extracellular matrix and exhibits a slightly acidic pH that provides endogenous stimuli for *in situ* self-assembly.[33–35] Other tissues and organs also have self-assembly stimuli-responsive factors, such as gene promoter driving in the liver and high flow shear force driving in blood vessels.[36,37]

2.1.1 The slightly acidic pH of the tumor microenvironment. The normal physiological environment has a pH of 7.4, whereas the extracellular matrix of the tumor microenvironment ranges from 6.5–7.4 due to the continuous transport of H^+ ions from inside to outside of the cell by ion-exchange proteins on the tumor cell membrane, which helps to prevent auto-acidosis. This leads to a slightly acidic environment in the tumor microenvironment, which various biomaterials take advantage of by self-assembling or reassembling into different morphologies that exert different physiological functions. For example, peptide nanomedicines can self-assemble into supercoiled structures under simulated neutral pH conditions *in vitro*, disassemble into NPs under weakly acidic pH conditions similar to the tumor environment, and re-form supercoils after endo/lysosome escape.[38–40] To achieve *in situ* pH-reversible self-assembly, Cheng *et al.*[40] designed the nanomedicine ACI, a peptide derivative that forms a supercoiled structure in an α-sheet conformation at pH 7.4. When ACI enters the tumor microenvironment (where the pH drops to 6.5), it transforms into an NP form, thanks to the pH-responsive morphological transition attributed to the amide bond of 4-aminoproline (Amp) in ACI, which undergoes *cis*-to-*trans* isomerization (Fig. 1A).[41] This reversible morphologically variable nanodrug system has a higher delivery efficiency than single morphology nanodrug systems, as the NPs can easily penetrate the cell membrane and the superhelix can prolong the circulation and increase the residence time in the blood circulation and cytoplasm, respectively.[42,43] Monitoring tumor growth through fluorescence imaging in animals can demonstrate a higher accumulation of superhelix structures in tumor tissue. Similarly, reversible conversion of nanofibers (NFs) and NPs is achieved in drug delivery processes, resulting in efficient delivery of IDO-1 inhibitors (a small molecule immune checkpoint blocker).[42,44] By functionalizing peptides with antigenic epitopes, two different forms of peptide vaccines can be prepared. Peptide vaccines with Amp can self-assemble into peptide NFs, which have a fibrillar

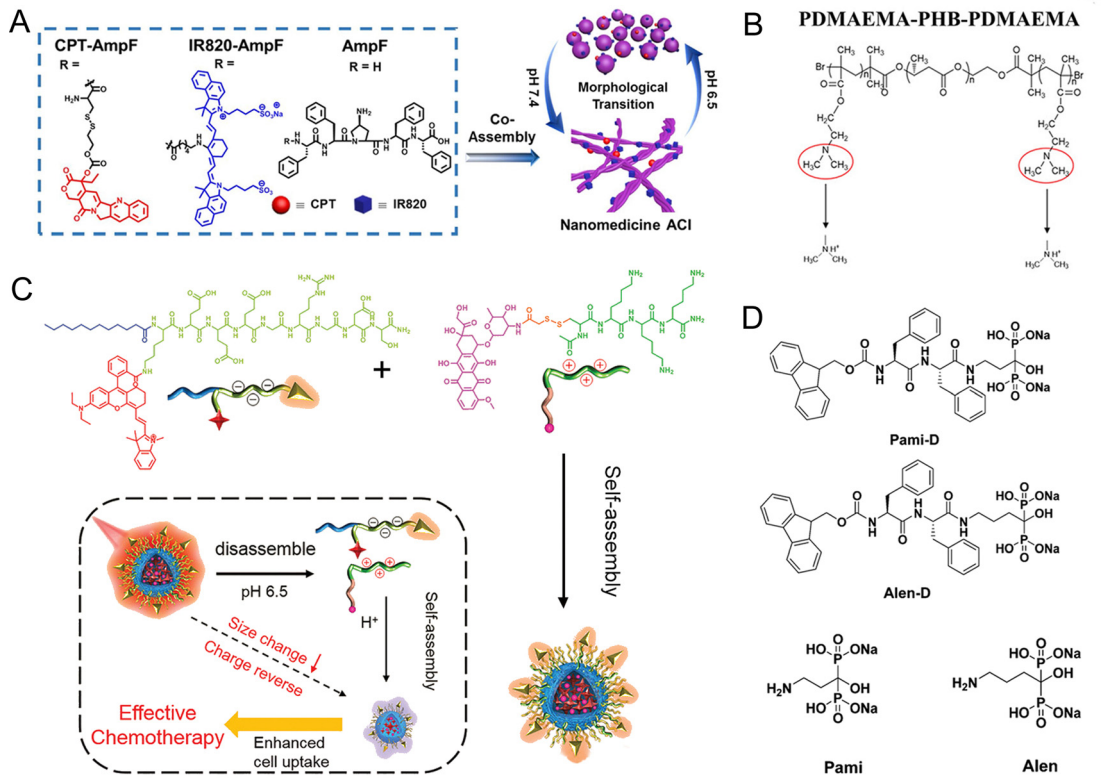

Fig. 1 (A) Molecular structure and pH-induced morphological transition of nanomedicine ACI.[40] Copyright 2020, Elsevier. (B) Polymer PDMAEMA–PHB–PDMAEMA with charge-reversal behavior.[47] Copyright 2020, WILEY-VCH. (C) The molecular structure of multifunctional bicomponent NPs and the formation process and size transformation driven by electrostatic interaction.[49] Copyright 2021, Wiley-VCH. (D) Chemical structures of Pami-D, Alen-D, Pami, and Alen.[55] Copyright 2021, The Royal Society of Chemistry.

structure that plays a crucial role in regulating cell–matrix interactions affecting cell adhesion, migration, proliferation, and *in vivo* drug response.[23] Compared to the peptide NP vaccine, the retention time of the peptide NF vaccine in dendritic cells is prolonged, leading to cell maturation, accumulation in lymph nodes, T cells infiltrating into tumor tissue, thus realizing the immune response of the peptide vaccine.[45]

NPs are typically neutral or negatively charged under a normal physiological environment, and thus remain stable in the bloodstream and are not taken up by macrophages. However, upon reaching the tumor site, a charge reversal occurs, making the NPs positively charged and allowing them to be attracted and taken up by negatively charged tumor cells.[46] For instance, chemotherapeutic drug doxorubicin (DOX) and photosensitizer ZnPc were attached to the polymer PDMAEMA–PHB–PDMAEMA to form charge-reversal-based pH-sensitive NPs, which self-assembled through π–π interaction and hydrophobic force. The tertiary amine group of the hydrophilic part of the polymer was protonated in the slightly acidic environment of the tumor (pH = 6.5), leading to a change in the NPs' charge potential from negative to positive (Fig. 1B). This change greatly enhanced the NPs' affinity with tumor cells and facilitated cellular uptake.[47] Similarly, a negatively charged pH-responsive polymer was modified at the outer shell through electrostatic interaction using a positively charged complex core composed of polyethyleneimine (PEI25K) and pDNA. The outer shell is removed under the slightly acidic pH conditions of the tumor, exposing the positively charged inner core to bind to the cell membrane.[48] Additionally, some self-assembly processes can be induced by electrostatic interaction. For example, Ma *et al.*[49] self-assembled negatively and positively charged peptides into NPs with a particle size of approximately 170 nm that had good stability through electrostatic interaction. Cell uptake experiments show that near-infrared (NIR) laser irradiation and acid environment triggered their disassembly and reassembly into smaller NPs (<30 nm), which were more likely to penetrate tumor cells and improve cellular internalization (Fig. 1C).[50]

The tumor microenvironment is characterized by high levels of extracellular H^+ and K^+. To deliver the anticancer aptamer AS1411, Peng *et al.*[51] designed a dimeric frame nucleic acid (FNA) based on pH-responsive self-assembly in living cells, using H^+- and/or K^+-responsive logic sensors. The branching apex of the FNA blocks AS1411, while a bimolecular i-motif serves as a control unit, enabling the FNA to respond to changes in extracellular H^+. K^+ facilitates the folding of AS1411 into a G-quadruplex for release from the dimeric FNA, resulting in fluorescence resonance energy transfer (FRET). Compared to the traditional delivery route, using FNA as a delivery system shows the strong transport ability of AS1411 and high targeting of the environment recognition response, with significantly increased delivery efficiency. This

approach has great potential for targeted drug delivery and accurate cancer therapy in the tumor microenvironment.[52–54]

In vitro simulation of acidic microenvironments in bone resorption voids showed that pamidronate (Pami)-derivative and alendronate (Alen)-derivative hydrogels self-assemble into NFs and subsequently form supramolecular hydrogels under acidic conditions (Fig. 1D). This self-assembly mechanism is similar to that in the slightly acidic environment of the tumor, where the salt is protonated and self-assembly occurs through electrostatic interactions. The self-assembled hydrogels exhibit a significantly enhanced inhibitory effect on osteoclasts, thereby improving bone resorption inhibition in a substantial manner.[55–58]

2.1.2 Specific enzymes of the tumor microenvironment. On the one hand, overexpression of certain genes in the disease site can greatly alter enzyme activity and expression, which have the advantage of high selectivity. On the other hand, many diseases begin with molecular failures too small to be detected by current diagnostic techniques. Designing self-assembly systems can be a solution that benefits disease detection and treatment. Using over-expressed enzymes in the tissue microenvironment as triggers for self-assembly and designing molecular structures for *in situ* self-assembly at the focal site can achieve drug delivery or better disease treatment.[59]

Matrix metalloproteinases (MMPs) are a ubiquitous family of extracellular matrix enzymes that are locally expressed at high levels in many types of solid tumors. The cancer-related enzyme MMP-7 cleaves the 16C alkyl group outside the cell, removing part of the peptide sequence and leaving a tetrapeptide fragment in the middle that can be used as both a hydrogen-bonded receptor and a donor to self-assemble with the adjacent 16C alkyl group (Fig. 2A).[60] The lysate of dead HeLa cells was collected, and the morphology of NFs was observed under a transmission electron microscope (TEM). The self-assembled NFs can kill cancer cells, amplify intracellular molecular-level events, and make drug resistance nearly impossible compared to traditional chemotherapeutics. Many studies are designing enzyme-sensitive drug delivery carrier systems in response to the tumor microenvironment MMP-2.[61,62] AuNPs are common drug delivery vehicles that can be coupled with various functional groups (such as peptides, DNA, and antibodies) to give them physiological responses, such as anti-tumor, anti-viral, and targeting abilities. Enzymatic self-assembly is achieved by coupling AuNPs with enzyme-sensitive peptides in the tumor microenvironment.[63–65] The DDS is injected into the body by intravenous injection and can accumulate in the tumor microenvironment due to the simultaneous enhanced permeability and retention (EPR) effect and the targeting function of RGD ligands. The peptides are then selectively cleaved by MMP-2 and self-assembled with adjacent NPs through intermolecular hydrogen bonds, and

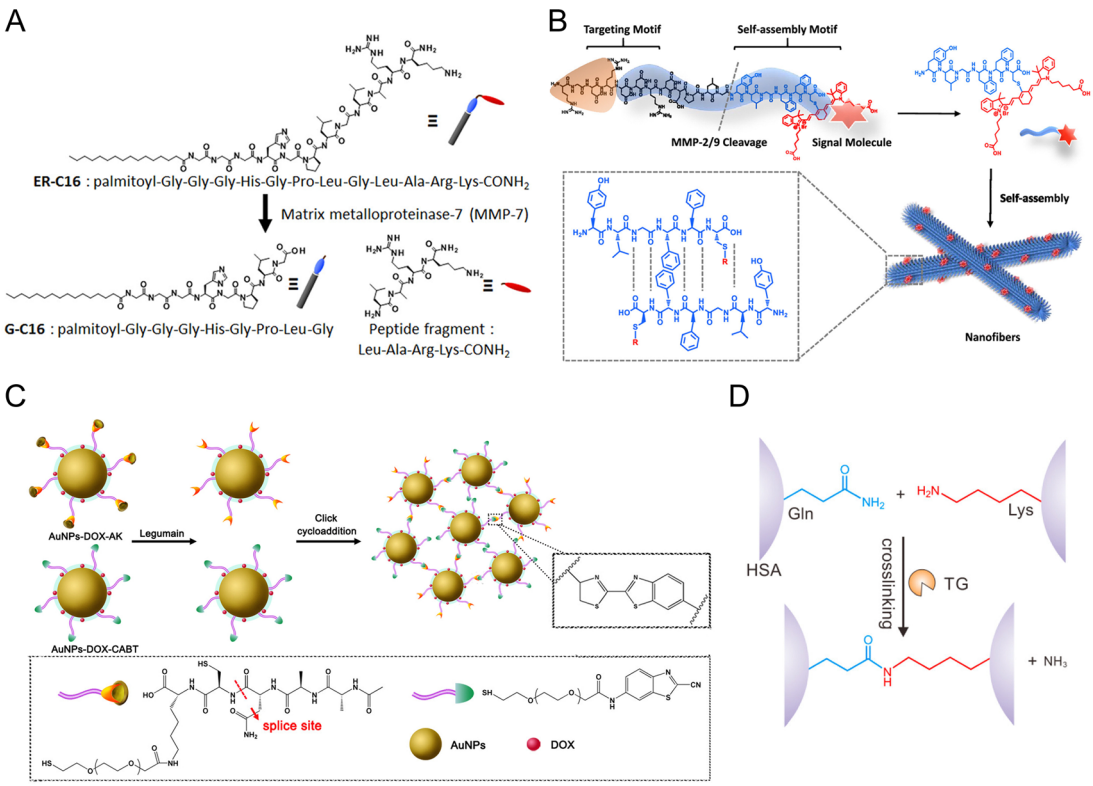

Fig. 2 (A) Molecular structure of the peptide sequence cleaved by MMP-7.[60] Copyright 2015, the American Chemical Society. (B) The modular molecular design includes (i) recognition motif, (ii) enzyme-responsive peptide linker, (iii) self-assembly motif, and (iv) signaling molecule and the self-assembly process cut by MMP-2.[67] Copyright 2020, the American Chemical Society. (C) Diagram depicting the legumain-triggered aggregation and composition of AuNPs-DOX-A&C.[69] Copyright 2016, the American Chemical Society. (D) TG catalyzes the cross-linking of Gln and Lys.[71] Copyright 2016, the American Chemical Society.

the aggregates exhibit enhanced retention effects that increase to approximately three-fold at 12 or 48 hours post-injection.[66] The peptide PLGYLG or KLVFF, which can be explicitly cleaved by MMP-2/9, serves as an enzyme-responsive motif. The residual molecules include self-assembly motifs and fluorescent functional motifs, which self-assemble through the intramolecular hydrogen bonds of the peptide to form β-sheet NFs, facilitating cancer cell retention imaging (Fig. 2B).[62,64,67] Hou *et al.*[68] reported an activated excretory-retarded tumor imaging (AERTI) strategy that can be activated by MMP-2 *in situ*. The strategy self-assembles in 786-O cells with positive MMP-2/9 expression, as confirmed by the gelatin zymography assay. After cutting the linker motif, the self-assembly peptide KLVFFGC is exposed, and hydrogen bonding-driven self-assembly occurs. However, since the system contains motifs targeting the cell surface receptor integrin $\alpha_V\beta_3$, self-assembly occurs at the tumor cell surface. The assembly principle of targeting $\alpha_V\beta_3$ is discussed in 2.2.2.

Legumain is an enzyme that can cleave the surface-modified AuNPs-AK, exposing a 1,2-mercaptoamino group, which undergoes a click cycloaddition reaction with adjacent cyano groups to form aggregates. This leads to enhanced retention of the aggregates in glioma cells, as demonstrated by *in vivo* photoacoustic imaging revealing the formation of *in situ* aggregates. To further improve the therapeutic efficacy, DOX is connected to AuNPs-A&C through pH-sensitive connectors, and the resulting drug-loaded NPs are self-assembled using the same principle to form AuNPs-DOX-A&C. This enhanced retention effect increases the utilization of DOX and exhibits a better therapeutic effect on gliomas. In comparison to the control group, the median survival time of DOX-coupled AuNPs-A&C increased by 288% in the experiments (Fig. 2C).[69,70]

In addition, the carrier made from hyaluronic acid (HA), coated with polymer, is degraded by hyaluronidase (HAase), an enzyme found in the tumor microenvironment that acts as a catalyst for the release of transglutaminase (TG). Subsequently, the amine and acyl groups on human serum albumin (HSA) undergo a click chemical reaction and cross-link to form a larger DDS, which can be degraded and released under acidic conditions (Fig. 2D). The increased size can effectively inhibit the internalization of the drug carrier and promote the interaction between the drug and the plasma membrane, thereby enhancing the synergistic anticancer efficacy.[71]

2.1.3 Other tissue microenvironments. Promoters can regulate various functions, including chromosome recruitment and promoter-specific co-assembly.[37] Currently, studies on the transcription of recombinant genes driven by cytomegalovirus (CMV) promoters have been used to produce recombinant proteins and viral vectors.[72] Using liver cells as the chassis, the host liver is reprogrammed to guide the synthesis and self-assembly of small-interfering RNA (siRNA) into secretory exosomes, thereby promoting siRNA delivery *in vivo*. Zhang's group utilized this *in vivo* siRNA delivery platform to target key pathogenic genes for lung cancer (EGFR/KRAS), glioblastoma (EGFR/TNC), obesity (PTP1B),[73] and Huntington's disease (mHTT),[74] with significant therapeutic effects observed. The genetic circuit reaches the liver through intravenous injection, and the CMV promoter drives specific siRNA transcription, self-assembling into an exosome with the siRNA loaded internally. At the same time, neuron-targeted RVG is assembled on the surface of the exosome. Compared to culturing cells and extracting exosomes or other extracellular vesicles, this *in vivo* self-assembly strategy uses human cells as a cell factory to produce secretory and medicinal small RNAs more efficiently and with better biocompatibility.

Under high shear stress conditions in blood vessels, the von Willebrand factor protein exerts hemostasis. At a certain shear rate, this protein undergoes a change from a contracted to a stretched state, exposing sufficient binding sites to adhere to the surface of the collagen matrix, forming a dense network that mediates platelet adhesion and further blood coagulation.[75] Wang's group[36] proposed a novel shear-driven *in situ* polymer self-assembly method that utilizes the shear force of the fluid to effectively and rapidly stretch the macromolecular chain, promoting adhesion. The method has the advantage of promoting the orderly arrangement of the adsorbed macromolecular species, optimizing the surface morphology and structural compactness of the assembled film. Furthermore, the *in situ* self-assembly method simplifies the operation, and a layer-by-layer assembly cycle can be completed in just two minutes.

2.2 Cell surface self-assembly

The actions on cell surfaces have attracted significant attention as they drive many cellular events, including cell adhesion, proliferation, and hormone uptake.[76] Enzymes and receptors are present in abundance on the cell surface, and actively targeting the cell surface by combining it with surface markers can enhance the efficiency of nano-carriers for delivering a variety of drugs into the cells, while also significantly reducing toxicity in the life system.[77] This can be achieved by combining molecular motifs targeting the cell surface with self-assembly motifs, leading to the self-assembly of the cell surface. Several studies have investigated this approach.[78,79]

2.2.1 Enzymes on the cell surface. It is well-known that cancer cell membranes overexpress alkaline phosphatase (ALP), carbonic anhydrase IX, and furin, compared to normal cell membranes. However, the cell membrane acts as a barrier preventing the free entry of extracellular substances, which makes it difficult for drugs or DDS to penetrate the cell membrane and enter the cell after reaching a certain molecular weight. To overcome this issue, designing nanomaterials that target the cell surface and self-assemble *in situ* can induce phase separation of the membrane, thereby improving the permeability of the cell membrane and increasing the uptake of macromolecular drugs.[80,81] Guo *et al.*[82] proposed a peptide, KYp, that can be stimulated by ALP on the surface of tumor cells. Subsequently, KYp removes the phosphate group, exposing the strongly hydrophobic benzene ring (Fig. 3A). Hydrophobic interactions provide the driving force for self-assembly to form NPs. ALP and NPs form a larger assembly, resulting in protein-lipid phase separation of the cell membrane and increased permeability. The result is that the peptide KYp directly enters the cell,

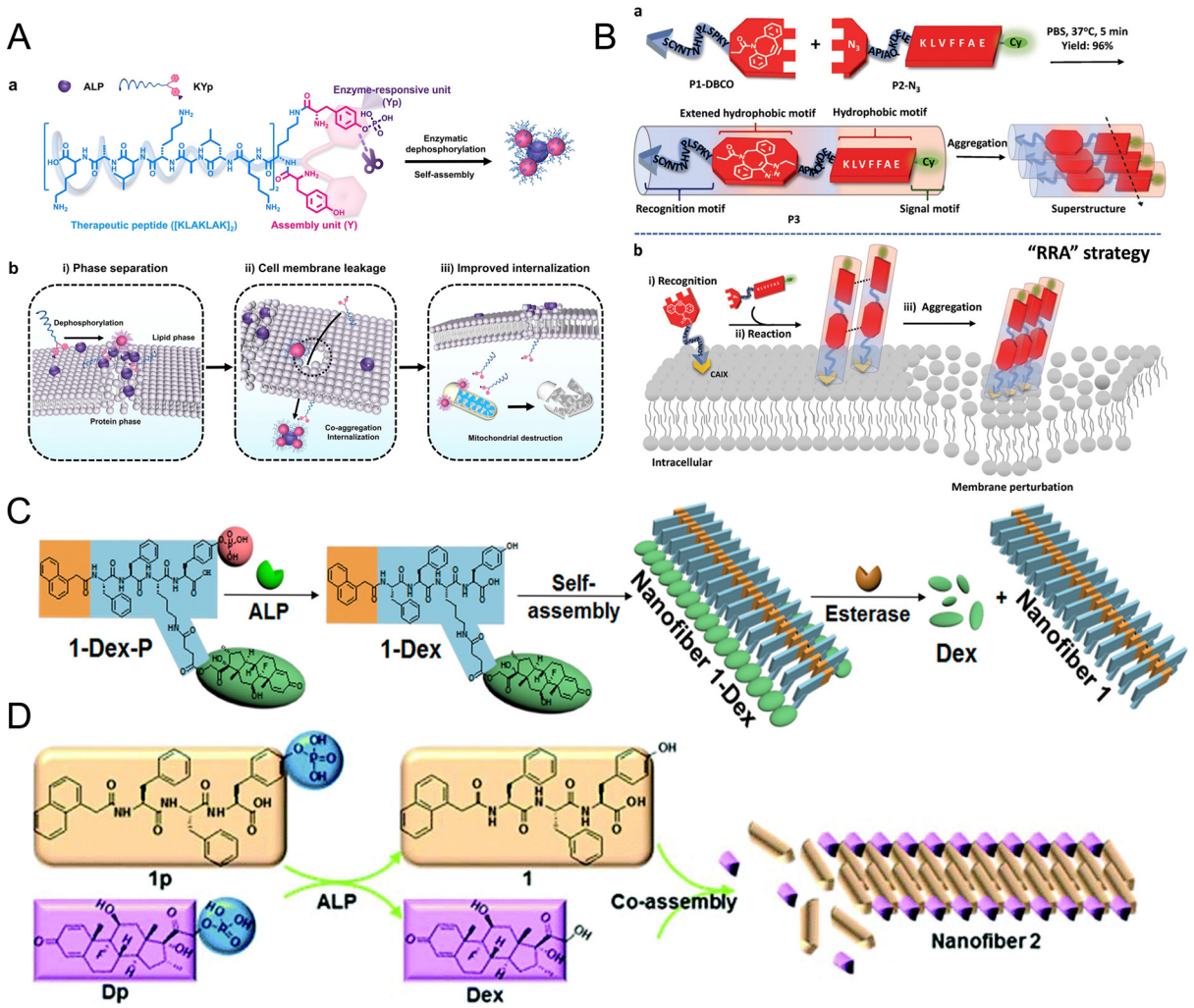

Fig. 3 (A) ALP responsive peptide and its self-assembly on the cell membrane. (a) KYp is stimulated by ALP to release phosphate groups and form aggregates with ALP. (b) (i) Phase separation of the protein and lipid phases; (ii) leakage of cell membrane; (iii) enhanced the internalization of peptides.[82] Copyright 2021, WILEY-VCH. (B) Schematic illustration of the molecular structure and the RRA cascade process. (a) P1-DBCO and P2–N3 generate P3 in PBS and self-assemble to form aggregates. (b) The process of *in situ* recognition, reaction and aggregation on the cancer cell membrane.[84] Copyright 2019, WILEY-VCH. (C) Schematic illustration of the self-assembly and drug release process of nanofiber 1-Dex.[86] Copyright 2018, the American Chemical Society. (D) Schematic illustration of ALP-instructed coassembly of 1p and Dp to form Nanofiber 2.[87] Copyright 2017, The Royal Society of Chemistry.

reaches the mitochondria, and induces mitochondrial apoptosis, resulting in a better tumor treatment effect.

The use of enzymes overexpressed by tumor cells to trigger self-assembly and induce phase separation for increased uptake of small molecule anticancer drugs has also been studied.[83] In one such study, Wang *et al.*[84] designed the peptide P1-DBCO, which can recognize CA IX on the membrane of renal cancer cells, and the peptide P2–N3, which can self-assemble by increasing hydrophobicity. The two peptides were combined through a chemical reaction, forming the peptide P3 superstructure that can adhere to the cell surface. P2–N3 has an azide group, a hydrophilic N-terminal sequence, and a hydrophobic signal-blocking aggregation sequence (KLVFFAE), showing a hydrophilic–hydrophobic balance. The newly formed nitrogen heterocyclic structure of P3 extends the hydrophobic motif, thereby breaking the hydrophilic–hydrophobic balance. Moreover, intermolecular hydrogen bonds trigger the aggregation of assembled sequences (KLVFFAE), which further form β-sheet structures at neutral pH.[85] The simulated cell membrane structure of giant plasma membrane vesicles (GPMVs) is disrupted, resulting in increased permeability and more DOX entry into renal cancer cells, improving drug utilization and sensitivity (Fig. 3B). In short, increasing cell membrane permeability can solve the problem of both macromolecular drugs and small molecules having difficulty passing through the cell membrane and can also address the drug resistance of small molecules, offering good prospects for drug therapy.

Self-assemblies anchored to the cell surface have shown potential as drug delivery vehicles for conventional chemotherapeutic drugs or anti-inflammatory agents. Platinum(IV) prodrugs with phosphate groups can respond to phosphatase and undergo self-assembly, transforming hydrophilic molecules into supramolecular structures with NF morphology on the surface of cancer cells. This approach enhances the cellular

uptake of cisplatin, resulting in high cancer cell selectivity and low cytotoxicity.[29] Tang and coworkers[86] designed an ALP stimuli-responsive hydrogel precursor, 1-Dex-P, which self-assembles into NFs 1-Dex after dephosphorylation (Fig. 3C). The anti-inflammatory drug dexamethasone (Dex) is released into cells by enzymatic hydrolysis and used to treat liver fibrosis in the development of chronic liver disease. *In vitro* and *in vivo* experiments demonstrated that 1-Dex-P has a more significant anti-fibrotic effect than the free drug. This enzyme-induced self-assembly of NFs for drug delivery can serve as a reference for designing more complex DDS. The hydrogel precursor (1p) and dexamethasone sodium phosphate (Dp) were dephosphorylated (p) under the stimulation of ALP on the cell surface. The two did not self-assemble immediately, but only until 1 and Dex entered the cell, respectively, and then self-assembled into NFs (Fig. 3D). The self-assembled DDS not only delivers Dex into cells but also prolongs the retention time and achieves slow release, thereby binding to the glucocorticoid receptor in the cytosol of macrophages, resulting in the attenuation of inflammatory molecule expression and improving the anti-inflammatory effect.[87] The self-assemblies themselves can also induce apoptosis by combining the self-assembly motif with a toxic effect due to their excellent retention effect. The self-assembled peptide sequence HAILLITKGIFK, derived from African snail mucus, has been shown to bind to and display cytotoxicity against MCF-7 breast cancer cells.[88]

Another study has shown that phosphopeptides can be dephosphorylated by ALP on the cell surface to produce peptide NFs for *in vivo* escape, resulting in decreased metabolic activity and cell death in the osteosarcoma cell line SaOs2.[89,90] Additionally, nanoscale assemblies formed by oligomers on cancer cell surfaces can enhance endocytosis and promote uptake by cancer cells.[91] Furthermore, ALP can dephosphorylate fluorescent molecular probes containing phosphate groups, which can self-assemble on the cell surface to form fluorescent aggregates that are decomposed by glutathione (GSH) upon reaching the cell, causing fluorescence to turn off.[92,93] The combination of self-assembly and fluorescence has been widely used in molecular imaging and tissue engineering to display biological processes more intuitively.[94–96] Cancer cells with high furin expression can induce peptide molecules containing the RVRR motif to self-assemble into β-sheet nanostructures in just five minutes in aqueous solution.[97] These nanostructures, linked with a furin protease-targeting peptide motif to the gelatinizable motif Nap-FF, selectively inhibit aggressive tumor growth and can be detected by fluorescence imaging (Fig. 4A).[98,99] Small molecule chemotherapeutics often require self-assembly to reduce toxicity.[100] The anticancer drug paclitaxel derivatives can be directly self-assembled to form NPs, which do not require an additional DDS for loading. Modified paclitaxel can be condensed under the stimulation of furin on the cell surface, self-assembled to form paclitaxel NPs, and then slowly released in the cell, significantly improving drug resistance without inducing cytotoxicity, since there is no introduction of exogenous substances as drug delivery carriers.[101]

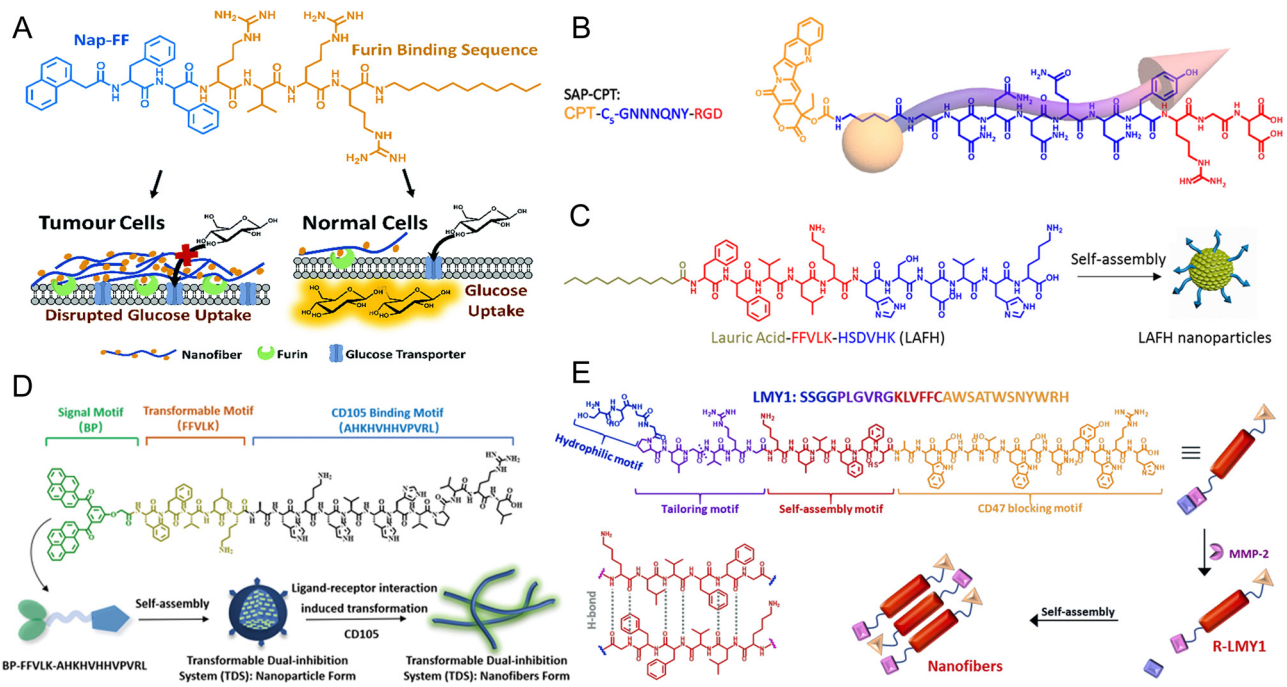

Fig. 4 (A) Molecular structure of the peptidyl furin inhibitor derivative and tumor enzyme affinity mediated molecular crowding for the selective disruption of glucose uptake.[98] Copyright 2018, The Royal Society of Chemistry. (B) The molecule structure of peptide conjugate drug SAP-CPT (CPT-C5-GNNNQNY-RGD).[102] Copyright 2021, Elsevier. (C) Molecular structure of LAFH and a cartoon of LAFH nanoparticles.[104] Copyright 2021, the American Chemical Society. (D) The structure of self-assembly peptide and TDS transformation.[107] Copyright 2020, WILEY-VCH. (E) The molecular structure includes a (i) targeting motif, (ii) MMP-2-responsive peptide linker, (iii) self-assembly motif and (iv) hydrophilic motif and a schematic illustration of the self-assembly process induced by MMP-2.[110] Copyright 2022, Elsevier.

2.2.2 Receptors on the cell surface. In addition to enzymes, cancer cells also overexpress a large number of receptors on their surface, and targeting these receptors can improve the precision of drug delivery or therapy. One example is the self-assembling peptide–drug conjugate SAP-CPT, in which the SAP molecule targets the integrin $\alpha_V\beta_3$ receptor overexpressed on the tumor cells' surface (Fig. 4B).[102] The hydrophobic dodecyl chain at the end of the peptide chain allows the monomers to self-assemble into peptide–drug nanoclusters *in situ*.[103] The advantages of nanoclusters include an increased maximum tolerated dose of drugs and improved drug bioavailability in cells. Interestingly, while single molecules have difficulty penetrating the nucleus, self-assembled nanoclusters can enter the nucleus more effectively through an endocytosis-like mechanism. The integrin $\alpha_V\beta_3$ receptor is also overexpressed on neovascular endothelial cells (ECs), which are associated with various diseases such as tumors, eye diseases, and Alzheimer's disease. By first self-assembling into NPs, single-targeting peptide-conjugated antibodies can then specifically bind to integrin $\alpha_V\beta_3$ and form a NF network. This network persistently captures integrins and covers other angiogenesis-related receptors, showing great anti-angiogenic potential (Fig. 4C and 5A).[104] NF networks on tumor cells can significantly block tumor cell-induced platelet agglutination *in vitro* and prevent platelet adhesion around circulating tumor cells (CTCs) *in vivo*, limiting the pro-metastatic effect of platelets and preventing early metastasis.[105]

Based on the verification of the peptide sequence targeting the integrin $\alpha_V\beta_3$ receptor, the targeted receptor can be replaced by a cluster of differentiation (CD), such as the CD3 protein, to obtain an enhanced self-assembly effect that promotes receptor oligomerization and T cell activation to exert immune effects.[106] Another potential target, CD105, can simultaneously inhibit tumor neovascular endothelial cells and tumor stem cells. After targeting the surface of the cell membrane, the self-assembly motif plays a major role in assembly. Peptide derivatives rely on hydrogen bonds to form network-like NFs through amide bonds, and when they cover the cell membrane, they act as a barrier and ultimately inhibit angiogenesis and cancer metastasis (Fig. 4D and 5B).[107] Chu *et al.*[76] used polymer conjugates with anti-CD20 antibodies to mimic immune effector cells to cross-link target cell surface receptors. Through a pair of single-stranded morpholino oligonucleotides (MORF1-MORF2) with complementary base sequences, the conjugates bind to CD20 receptors on the surface of malignant B cells and then hybridize and self-assemble to induce apoptosis (Fig. 5D). Moreover, conjugating anti-CD20 aptamers to macromers can efficiently and stably target self-aggregation/assembly on the surface of Raji cells due to the ligand–receptor interaction under the stimulation of ammonium peroxysulfate (APS). As a result, CD20 receptors are induced to aggregate, thereby

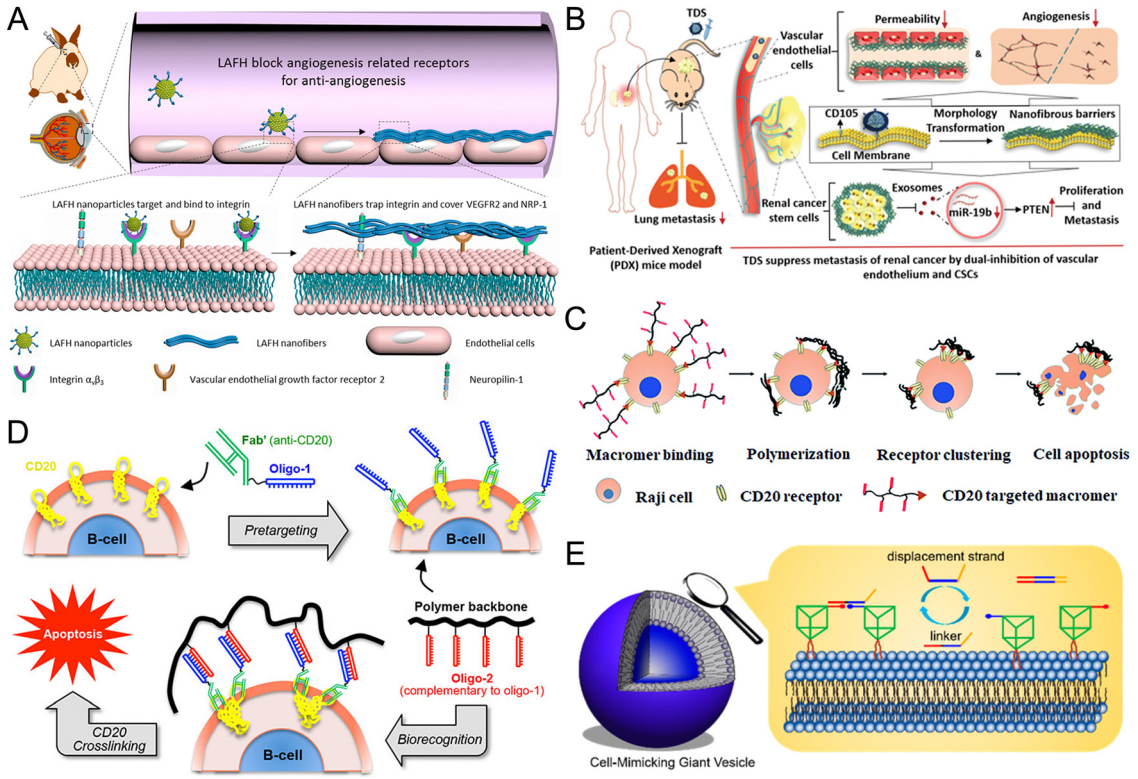

Fig. 5 (A) A schematic illustration of contact of LAFH NPs and integrin $\alpha_V\beta_3$ to form LAFH NFs.[104] Copyright 2021, the American Chemical Society. (B) Nanofibrous barriers formed by TDS suppress metastasis of renal cancer by dual inhibition of vascular endothelium and CSCs.[107] Copyright 2020, WILEY-VCH. (C) Cell-surface polymerization induced CD20 receptor clustering, thus causing the apoptosis of Raji cells.[108] Copyright 2020, The Royal Society of Chemistry. (D) CD20-mediated self-assembly of cell membrane (hybridization of MORF1-MORF2).[76] Copyright 2014, the American Chemical Society. (E) Assembly/disassembly of DNA nanostructures anchored on MVs.[112] Copyright 2017, the American Chemical Society.

triggering apoptosis (Fig. 5C).[108] In this approach, monomers work independently and bind to cells before being triggered to self-assemble into multimers, which are further endowed with greater viability and additional functionalities.[109] Such cell-surface receptor cross-linking can be applied to modulate the fate and function of other cells, especially those mediated by the spatial distribution of cell-surface receptors. For example, self-assembly targeting CD47 receptors leads to T cell activation. When the molecules are anchored to the CD receptors on the cell membrane, the conditions for the self-assembly effect also require the participation of enzymes in the microenvironment. The molecular structure is designed with four motifs, including (i) AWSATWSNYWRH as a CD47 targeting motif, (ii) PLGVRG as an MMP-2 reactive peptide ligand, (iii) KLVFFC as a self-assembly motif, and (iv) SSGG as a hydrophilic motif. After being cut by MMP-2, the molecule (LMY1) becomes a residual molecule (R-LMY1). The hydrogen bond of the peptide sequence drives the molecule to self-assemble into NFs (Fig. 4E). Finally, the "Eat Me" signal of macrophages is activated by MMP-2 cutting and targeted blocking of CD47.[110] The designed treatment is free of small molecule cytotoxic compounds and is designed to improve chemotherapy, radiotherapy, and immunotherapy. Based on rolling ring amplification (RCA) and three single-stranded DNA, the "Willow Branch" DNA (WB DNA) assembly was constructed. With the binding of CD44 antibody and S2.2 aptamer to the receptor on the cell membrane, the RCA scaffold successfully assembled WB DNA, achieving dual targeting and value-added inhibition of cancer.[111] Therefore, CD receptor-mediated self-assembly has research value in cancer therapy or combined immunotherapy.

Dynamic DNA nanotechnology involves the study and application of toehold-mediated nucleic acid chain replacement reactions.[78] Peng *et al.*[112] used micron-sized giant membrane vesicles (MVs) to mimic living cell membranes and investigate the self-assembly and self-disassembly mechanisms of DNA prisms on the cell membrane. They efficiently localized three-dimensional DNA nanoprisms with DNA arms and cholesterol targets on the membrane surface. The dynamic manipulation of the assembly and disassembly of three-dimensional nanoprism was achieved through toehold-mediated DNA strand hybridization and DNA strand displacement reactions (Fig. 5E). A toehold is a single-stranded segment of DNA to which the invader strand can bind to initiate branch migration. The use of toeholds enables the construction of enzyme-free DNA reaction networks that exhibit complex dynamic behavior.

Grid proteins self-assemble on biofilms, promoting the fundamental process of endocytosis. Liposomes are artificial membranes that can fuse with cell membranes and are commonly used as drug delivery carriers.[113] Inspired by the structure of protein building blocks and grid protein self-assembly, researchers have designed a method to create DNA-coated liposomes by hydrophobically anchoring them and then linking them to the triskelion structure based on DNA on the liposome surface, resulting in advanced hybrid nano-carriers.[114]

2.3 Intracellular self-assembly

In situ self-assembly can be initiated by triggering intracellular conditions or by interacting with intracellular biomolecules. When combined with therapeutic drugs or luminescent functional molecules, nano-assemblies can enable intracellular drug delivery or image-assisted therapy. Simultaneous cancer monitoring and treatment can prevent overtreatment or undertreatment.

2.3.1 Intracellular enzymes. The tumor cells contain various heterogeneous enzymes, including carboxylesterase (CES), X-linked inhibitor of apoptosis protein (XIAP), caspases, and others. Although the monomer itself can penetrate cells well and diffuse, its low stability and vulnerability to enzymatic degradation *in vivo* under physiological conditions impede its further development as a drug or delivery vehicle. Therefore, researchers have proposed a solution to intracellularly assemble monomeric molecules into supramolecular materials that exhibit significantly improved accumulation and retention in tumor cells, thereby enhancing their therapeutic potential.[115]

The peptide fragments containing ester bonds are hydrolyzed by intracellular esterases. The hydrophilic hydroxyl groups and hydrophobic naphthyl groups exposed on the fragments provide hydrogen bonding and hydrophobic interactions, respectively, resulting in self-assembly in aqueous solution and hydrogelation, which can regulate cell death.[116] If the ester bond is replaced by an amide bond with a similar structure, it cannot be hydrolyzed and self-assembled. The precursors of small molecular peptides enter tumor cells, where CES cleaves the ester bond. The exposed hydroxyl groups provide the driving force for hydrogen bonding, and NFs self-assemble directly in aqueous solution.[117,118] Co-incubation with cisplatin significantly increases the activity of cisplatin against drug-resistant ovarian cancer. Under the catalysis of ALP and hydrolysis of CES, the functional molecules undergo a transformation to form nano-brush-NPs-NFs, and the conjugation of 2-(naphthalene-2-yl)acetic acid at the N-terminal of the nanogroup further enhances self-assembly through aromatic-aromatic interactions (Fig. 6A). Loaded with camptothecin, a chemotherapeutic drug, and hydroxychloroquine, used to inhibit autophagy, the nano-assemblies are released at specific sites. The intracellular NF morphology effectively inhibits the metastasis and invasive behavior of cancer cells.[119]

An *et al.*[120] built a system that loaded four fragments of tumor-specific recognition motifs, enzymatic cleavage linkers, self-assembly motifs, and functional drug molecules. When the system reaches the tumor cells, it is stimulated by XIAP, which is specifically expressed in the tumor cells. The enzyme cleaves the peptide bond between the linker and the self-assembly motif, and the newly formed peptide chain with the drug undergoes β-folding under the action of hydrogen bonds, and self-assembles to form a superfibrous structure (Fig. 6B). This system has been applied to the detection and treatment of bladder cancer.

Caspase 3/7 is a critical biomarker for tumor cell apoptosis. Once the Fe_3O_4@1 NP small molecule enters caspase 3/7-activated cells (*e.g.*, apoptotic HepG2 cells), the intracellular GSH reduces the disulfide bond in its cysteine motif, exposing reactive 1,2-aminothiol groups on the cleaved peptide substrate by caspase 3/7. Then, the free 1,2-aminothiol group undergoes

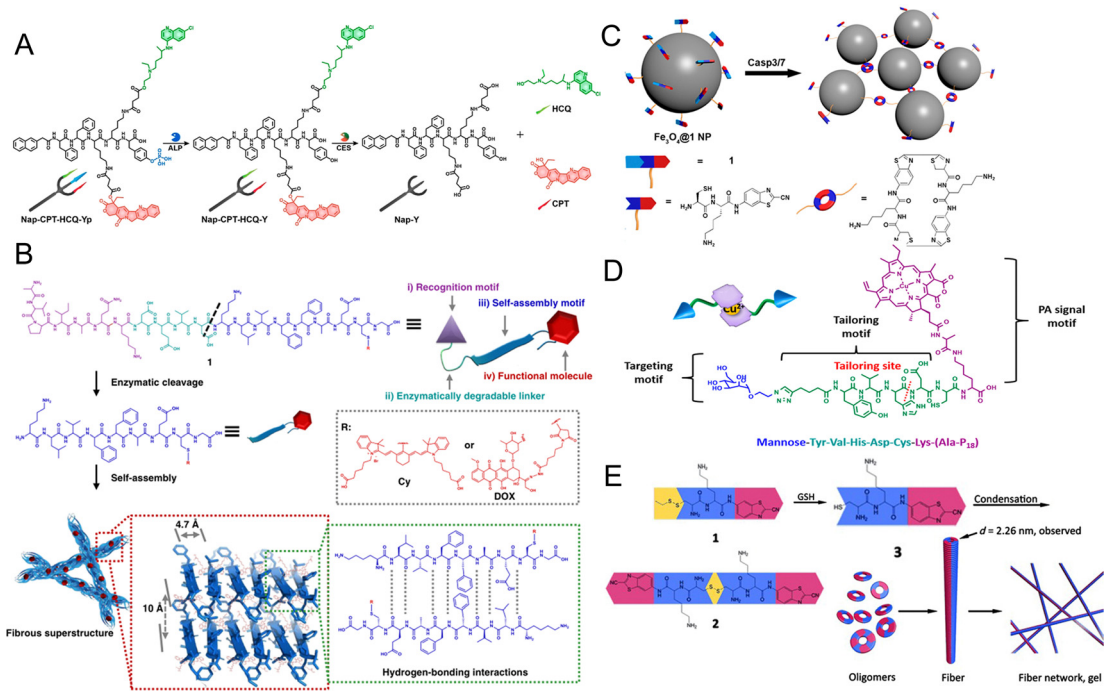

Fig. 6 (A) Chemical structures of Nap-CPT-HCQ-Yp and its enzymatic transformations.[119] Copyright 2022, the American Chemical Society. (B) The peptide molecular motif (i) recognition motif; (ii) enzymatically degradable linker; (iii) self-assembly motif; and (iv) functional molecule.[120] (C) Casp 3/7-instructed aggregation of Fe_3O_4@1 NPs.[121] Copyright 2016, the American Chemical Society. (D) Composition and chemical structure of Mannose-Tyr-Val-His-Asp-Cys-Lys-(Ala-P18).[122] Copyright 2018, the American Chemical Society. (E) GSH-controlled condensation reactions to yield cyclic amphiphilic oligomers which self-assemble into nanofibrous networks to form oligomeric hydrogels.[127] Copyright 2015, WILEY-VCH.

a condensation reaction with the cyano group of the cyanobenzothiazole (CBT) motif, leading to the formation of cross-linked Fe_3O_4 NP aggregates (Fig. 6C). Large magnetic NPs or aggregates have better magnetic resonance properties than ultra-small superparamagnetic iron oxide NPs, as they significantly reduce the transverse relaxation time (T2) of surrounding water protons, thus resulting in a T2-enhanced magnetic resonance signal.[121] Peptide YVHDC acts as a response motif to activate caspase-1 cleavage, with the clipping site located at the peptide bond between two amino acids. The retained P18-AL derivative exposes the hydrophobic amino group, which provides the driving force for self-assembly, and the formed nano-assembly is two times stronger than the original photoacoustic signal (Fig. 6D).[122]

2.3.2 Redox. The intracellular environment of tumor cells is characterized by high levels of GSH and reactive oxygen species (ROS).[123] Peptide precursors containing disulfide bonds can be reduced by GSH, exposing active 1,2-aminothiol groups that can undergo a click condensation reaction with the adjacent CBT molecule to form a cyclic dimer. Due to their amphiphilicity, these dimers can further self-assemble into NFs, resulting in higher mechanical strength and significant advantages in drug release compared to NFs directly self-assembled from monomers.[124,125] Small molecular peptides containing CBT and benzyl nitrocarbamate undergo GSH reduction and nitroreductase (NTR) cleavage, followed by click condensation to self-assemble into NPs. Intracellular NP formation can be directly observed by nano-computed tomography (nano-CT), providing deeper insight into the formation mechanism of small intracellular molecule nanodrug self-assembly.[126] Liu *et al.*[127] designed two hydrogel precursors containing disulfide bonds and CBT, which upon GSH stimulation undergo a click chemistry reaction, reducing disulfide bonds and self-condensing to produce cyclic dimers that immediately self-assemble into oligomeric hydrogel NFs (Fig. 6E). Oligomeric hydrogels offer the advantages of high mechanical strength of polymer hydrogels and the good biocompatibility and easy degradation of small molecular hydrogels, making them promising for drug delivery and long-term drug release.[128,129] Using the high GSH content in cancer cells for stimulation can achieve the self-assembly of lesions in the body and enable precise treatment.[130] However, since normal cells in cancer patients also contain GSH, chemotherapeutic drugs can reach normal cells and cause inevitable damage to the human body.[131] Therefore, GSH stimulation usually requires combination therapy or the design of nanodrugs that respond to multiple stimuli.

Tumor cell mitochondria are known to have higher levels of endogenous reactive oxygen species (ROS).[132] In the conjugate of the polymer and the cytotoxic peptide KLAK, the cleavage of the thioketal occurs under the trigger of ROS. This results in the destruction of the hydrophilic PEG and the breaking of the hydrophilic/hydrophobic balance. The hydrophobic force then becomes greater than the hydrophilic force, leading to the transformation of the NPs into NF structures with prominent KLAK. This delivery of cytotoxic peptides only targets cancer cells, resulting in better therapeutic effects.[133] ROS induces the formation of polymeric disulfides in the mitochondria of cancer cells, and due to the reductive intracellular environment, this

polymerization rarely occurs elsewhere in the cell. The polymerization of mercaptan monomers further increases the level of ROS in mitochondria, which automatically catalyzes the polymerization process and produces a fibrous polymer structure. This process can lead to mitochondrial dysfunction, which in turn activates necrotic apoptosis. Therefore, this *in situ* autopolymerization system shows great potential for cancer treatment, including drug-resistant cancers.[134] Considering the hypoxia-specific redox state and oxygen concentration, the hypoxia-sensitive chemical group nitroimidazole is designed to be a hypoxia-sensitive probe where the nitro group changes to hydroxylamine and binds to the mercaptan of cysteine. The self-assembly and aggregation effects of iron oxide NPs can be realized by modifying nitroimidazole on the surface of ultra-small iron oxide. This modification can achieve hypoxic tumor imaging by coupling fluorescent molecules. Experiments show that the self-assembly effect can amplify the imaging signal.[135,136]

The overexpression of hydrogen peroxide (H_2O_2) in the microenvironment of infected wounds (100–250 μM) makes it a useful marker for diagnosing wound infection.[137] In a recent study, Wang *et al.*[138] successfully activated *in situ* conjugate polymerization of aniline dimer derivatives in calcium alginate (CA) hydrogels for the first time using endogenous H_2O_2 in the wound infection microenvironment. The hydroxyl radicals ($^{\bullet}OH$) generated by H_2O_2 can trigger polymerization, enabling real-time detection of wound infection and bacterial inhibition.

In addition, it is known that polyamines are highly expressed in cancer cells, whereas non-tumor cells in the tumor microenvironment express them less. In the peptide derivative-drug conjugate, the first step involves self-assembly into NPs, which after internalization into polyamine-overexpressing cancer cells, undergo competitive dissociation of the outer hydrophilic end structure. The released peptide-camptothecin then readily forms a β-sheet structure, followed by the formation of microfibrillar structures. The morphological transformation from NPs to microfibrillar structures is beneficial for improving selective drug accumulation and retention within cancer cells.[139]

2.3.3 Low pH in lysosomes. As mentioned earlier, the tumor microenvironment has a weakly acidic pH range of 6.5–7.4, while lysosomes within tumor cells are acidic organelles with a pH range of 4.0–5.5.[140] i-DNA, also known as i-motif DNA, is an atypical quadruplex nucleic acid structure formed by cytosine-rich sequences, discovered in 1993. The multi-segment cytosines in i-motif DNA are partially protonated under acidic conditions (pH 5.0). Due to the Watson–Crick base pairing mechanism, C:C+ base pairing is generated to drive single-stranded DNA (ssDNA) to form a quadruplex. This pH-triggered conformational change of i-motif DNA has been utilized to modulate the assembly of AuNPs through pH changes.[141] When i-motif DNA is loaded onto AuNPs, the complementary recognition of ssDNAs and the pH sensitivity of i-motif DNA fold into a closed quadruplex. At the endosomal acidic pH, i-motif DNA-linked AuNP clusters can be used to deliver siRNA. Endosomal escape occurs, resulting in high gene silencing efficiency by releasing siRNA into the cytosol.[142] The DNA tetrahedra formed by the self-assembly of i-motif DNA can reversibly open/close DNA cages according to the pH value and are widely used as delivery vehicles. The encapsulated functional molecules can realize intelligent responses through encapsulation or release.[143]

Amino acid-functionalized amphiphilic perylene diimide (PDI) derivatives can also utilize the low pH of cancer cell lysosomes to stimulate self-assembly. Under physiological conditions, PDI derivatives exist as monomers or oligomers that can penetrate the cytoplasmic and lysosomal membranes. Once exposed to an acidic environment close to the lysosomal cavity, carboxylates undergo protonation. This protonation shields the electrorepulsion between carboxylates and leads to the aromatic accumulation of PDI, as well as self-assembly *via* hydrogen bonds between carboxyl groups, forming a strong fibrous structure. The structure of self-assembled fibers contributes to the rupture of lysosomes, which leads to cell death.[144]

In summary, the ultimate goal of drug delivery systems is to be used in animals or even humans. *In situ* self-assembly usually has the advantage of prolonging the residence time of drugs in the lesion. Therefore, we have summarized the drug delivery types and delivery methods of different self-assembled materials to enable researchers to evaluate drug delivery efficiency. The delivery efficiency can be considered maximized if the component performing the therapeutic action is itself. However, due to the complexity of the tissue microenvironment, cell surface, and intracellular environment, detecting self-assembly is difficult. Verification experiments are usually carried out *in vitro* to simulate conditions similar to the *in vivo* environment, as achieving real self-assembly in animals is challenging. *In situ* self-assembly tests *in vivo* are usually visualized using fluorescence detection (Table 1).

2.4 Exogenous stimuli

Designing controllable *in situ* self-assembly is challenging due to the complexity of endogenous stimuli in the *in vivo* physiological environment, which makes manual intervention and direct monitoring difficult. Therefore, exogenous stimuli intervention or combining endogenous stimuli are often considered as strategies to achieve control over the self-assembly process.

2.4.1 Light. Macromonomers have been shown to undergo free radical polymerization and self-assembly to form polymers. To fully exploit the advantages of monomers and aggregates, exogenous stimuli or combinations of endogenous stimuli can be applied to design controllable *in situ* self-assembly *in vivo*. For instance, photoinduced free radical polymerization was used to induce the aggregation of biocompatible methyl ferrocene methyl acrylate (FMMA), hydroxyethyl methacrylate (HEMA), and *N*-(2-hydroxypropyl)methacrylamide (HPMA) monomers into NPs *in situ* (Fig. 7A). The monomer HPMA and the initiator were added to the cell culture, with photopolymerization initiated by illumination at 365 nm. The self-assembled aggregates promote actin polymerization and regulate cell fluidity.[145] The intervention of exogenous light is a necessary condition for intracellular free radical polymerization. By adding fluorescent groups to generate functional polymers inside cells to manipulate and monitor cell behavior, the tedious synthesis and solution

Table 1 Drug delivery types, drug delivery methods and sites for *in situ* self-assembly testing of self-assembled materials

Self-assembling materials	Drugs in DDS	Delivery method	Test self-assembly *in vitro*	Test self-assembly *in vivo*	Ref.
Peptide	Camptothecin (CPT) and photosensitizer new indocyanine green IR820	Chemical conjugation	Solution, cell culture	Fluorescent imaging to demonstrate accumulation at tumor sites	40
Peptide	Human papillomavirus E7 protein antigen	Epitopes derivation	Solution, cell culture	Fluorescent imaging to demonstrate lymph node accumulation	45
Peptide	NIR dye, DOX	Chemical conjugation	Solution, cell culture	Self-assembly not demonstrated *in vivo*	49
Polymer	Functional proteins and functional peptides	Core-shell loading	Solution, cell culture	Fluorescent imaging to demonstrate accumulation at tumor sites	71
Peptide	Therapeutic peptide	Chemical conjugation	Solution, GPMVs, living cells	Fluorescent imaging to demonstrate accumulation at tumor sites	82
Peptide	Cyanine, DOX	Nucleophilic substitution reaction, cellular uptake	GPMVs	Fluorescent imaging to demonstrate accumulation at tumor sites	84
Peptide	Dexamethasone	Chemical conjugation	Enzyme and cell experiments	Self-assembly not demonstrated *in vivo*	86
Peptide	Dexamethasone	Chemical conjugation	Solution, cell culture	—	87
Small molecules	Cisplatin	Chemical conjugation	Solution, cell culture	Drug accumulation experiments to demonstrate long-term retention	29
Small molecules	Taxol	Chemical conjugation	Solution, cell culture	Self-assembly not demonstrated *in vivo*	101
Peptide	CPT	Chemical conjugation	Solution, cell culture	Self-assembly not demonstrated *in vivo*	102
DNA	—	Strand hybridization and strand displacement	GPMVs	—	112
Peptide	Fluorophore	Chemical conjugation	Solution, cell culture	—	117
Small molecules	CPT, hydroxychloroquine	Chemical conjugation	Solution, cell culture	Self-assembly not demonstrated *in vivo*	119

processing procedures of block copolymers in traditional self-assembly strategies can be avoided.[146,147]

Ocyanine-based photoacids are often used as light-responsive media. When exposed to visible light, the medium decreases its pH value and induces DNA triplex formation, leading to the spatial reconstruction of chiral plasma molecules.[148] *In vivo*, dynamic plasma nanostructures with adequate responses to different stimuli are prepared simultaneously using light radiation and multiple endogenous stimuli. Nanosystems based on DNA origami-linked gold nanorods (GNRs) with geometric shapes and chiral signals respond to multiple stimuli, including GSH reduction, restriction enzyme action, pH changes, or light irradiation. The control strand (green) contains the telomeric DNA sequence and forms a G-quadruplex with the light-regulating azobenzene moiety (blue). Upon UV irradiation, the *cis*-azo compound dissociates from the telomeric DNA control strand, and the folded G-quadruplex is stretched, leading to a larger inter-nanorod separation. Under visible light irradiation, the controller DNA refolds into a G-quadruplex with the help of the *trans* form of the azo, leading to smaller inter-nanorod separation (Fig. 7B).[149] Such light-driven DNA nanodevices can be used to manipulate materials or gather information, with a wide range of applications in biomedicine and micro/nano fields.[150,151] Currently, photosensitizers used in clinics are derivatives of porphyrin, dihydroporphine, and phthalocyanine (Pc),[152,153] which have edge or axial modifications. Only conditions triggered by light make it impossible for DDS to accurately target the lesion, therefore, it is necessary to introduce endogenous stimuli. Once assembled, DDS can typically extend the residence time and enhance the therapeutic effect of the drug.[154] Linking photosensitizers to self-assembling monomers (*e.g.*, peptides, aptamers, *etc.*) can trigger *in situ* self-assembly and apply photodynamic therapy to tumor therapy.[155] Self-assembled pentalysine-Pc assembly nanodots (PPAN) are formed by aggregating part of the hydrophobic Pc as a core and exposing part of penta-lysine to the physiologically hydrophobic conditions on the surface (Fig. 7C). The significantly increased molecular size prolongs the circulation period of photosensitizers *in vivo*.[156] Additionally, aggregation-induced emission luminogens (AIEgens) have been extensively studied in self-assembly imaging.[157,158] By binding AIEgens to self-assembled peptides, fluorescence is turned on after assembly due to hydrogen bonding driving the formation of secondary structures. Targeting the bacterial surface to exert anti-infective effects and enhance ROS production represents a potential strategy for disease diagnosis and treatment.[159] Self-assembled NPs have smaller polydispersity index (PDI) values, better inter-batch consistency, and long-term colloidal stability, which implies better potential for bioimaging.[157] The NIR-II fluorescence imaging properties of AIE NPs enable high-resolution imaging of superficial blood vessels through scalp and skull imaging of cerebral vessels and centimeter-level depth imaging of arteries.[160]

NIR laser-guided *in situ* self-assembly is a promising approach to overcome the challenges of poor permeability and low accumulation efficiency in tumor tissues.[161] To achieve this, functional peptides coupled with NIR molecules possessing photothermal properties are combined with a thermal response skeleton poly (β-thioester), which has a smaller size (<10 nm) at body temperature and can penetrate deeply into the tumor.[162] However, when irradiated with NIR, the temperature increases, leading to the self-assembly of whole thermal responsive molecules in the tumor. The resulting spherical NPs can accumulate in the tumor, effectively enter cells, and induce apoptosis by destroying the mitochondrial membrane (Fig. 7D).[163] By utilizing exogenous stimuli to control self-assembly, the instability

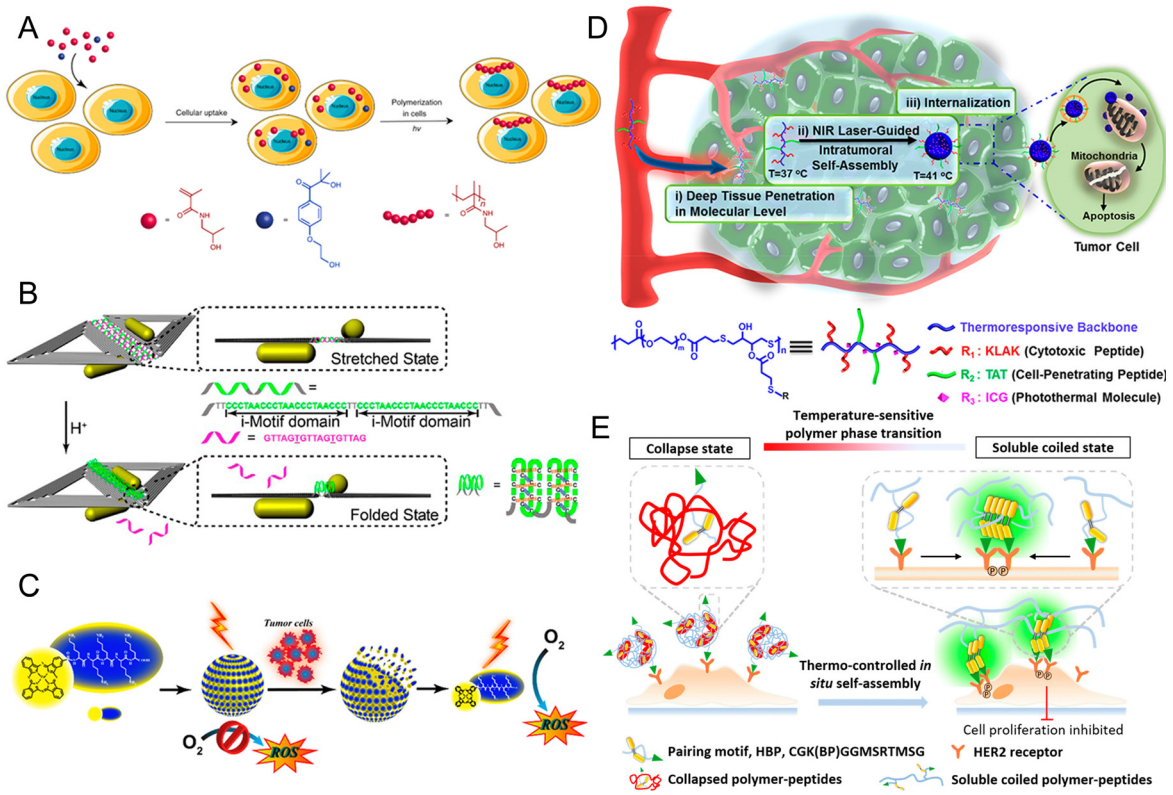

Fig. 7 (A) The monomer HPMA and the initiator were added to the cell culture, with photopolymerization inside living cells initiated by illumination.[145] Copyright 2019, Springer Nature. (B) Schematic illustration of the pH-response mechanism. The controller strands (green) are designed to contain the i-motif sequence and form duplexes with the complementary strands (pink). The pH acidification results in the folding of the linker strand into an i-motif, which results in smaller internanorod separation.[149] Copyright 2017, the American Chemical Society. (C) Self-assembly of PPAN under physiological hydrophilic conditions and disassembly in tumor cells.[156] Copyright 2018, the American Chemical Society. (D) Deep tissue penetration of polymer-peptide conjugates (PPCs) and the NIR laser induced *in situ* self-assembly.[163] Copyright 2018, the American Chemical Society. (E) Temperature-controlled aggregates on the cell surface for manipulating and monitoring HER2 receptor clustering.[167] Copyright 2016, the American Chemical Society.

and uncontrollability of the endogenous microenvironment can be circumvented, allowing the reaction to be activated or deactivated at any given time. When combined with endogenous stimuli to induce *in situ* self-assembly, the size of NPs can be precisely controlled at a specific location, providing the advantages of deep tumor infiltration, enhanced accumulation, and internalization of cells *in vivo*, thereby demonstrating extensive potential for tumor therapy.[162,164]

2.4.2 Temperature. The temperature-sensitive block molecules undergo a phase transition when the temperature is either higher or lower than the critical temperature, resulting in the provision of either an aqueous environment or hydrophobic fragments that are required for self-assembly.[165]

Bispyrene (BP) molecules, which are non-fluorescent in their monomeric state, can exhibit fluorescent effects when they self-aggregate into NPs in aqueous solutions due to their hydrophobicity and π–π interactions.[166] This fluorescence effect is commonly utilized to monitor the self-assembly/disassembly processes both *in vitro* and *in vivo*. Qiao *et al.*[167] employed thermoresponsive polymers to modulate the self-assembly of BP. Specifically, they used a temperature-sensitive polymer, poly(*N*-isopropylacrylamide) (PNIPAAm), as a thermoresponsive backbone that was covalently linked to HER2-targeting peptide-conjugated BP. The PNIPAAm polymer demonstrated a sharp water phase transition when heated above the critical temperature.[168] At 40 °C, the polymer collapsed, acting as a "shield" to prevent the aggregation of BP, whereas at 35 °C, the polymer stretched and exposed BP to the aqueous solution, leading to aggregation with a six-fold enhancement in fluorescence. When the polymer containing BP was incubated with living cells and the temperature was reduced from 40 °C to 35 °C, BP was able to target the surface aggregation of HER2 overexpression in cells (Fig. 7E).

The hydrophilic thermal response block oligomeric ethylene glycol monomethyl ether (OEG) chains to undergo dehydration at high temperatures, causing them to transition from a water-soluble crimped state to an insoluble spherical state.[169,170] OEG is linked with the hydrophobic core to form an amphiphilic structure, and the thermal response leads to a phase transition from microscopic self-assembly to macroscopic aggregation, thus enabling the visualization of the dynamic stimulus-response behavior of self-assembly.[171]

3. Conclusions

In a diseased state, the secretion and metabolism of cells differ from those of normal cells. Therefore, identifying the signal

Table 2 Summary of self-assembled materials with *in situ* stimulation response

Trigger position	Stimulating response factor	Assembly material	Driving force	Assembly result	Applications	Advantages	Ref.
Tumor microenvironment	pH	Peptide	Hydrogen bond, isomerization, electrostatic interaction	Supercoil, nanoparticles, nanofiber	Drug delivery, immunotherapy	Prolonged cycle and retention time, increased cell membrane penetration	40, 45 and 49
		Polymer	π–π stacking, hydrophobic effect	Nanoparticles	Drug delivery	Increased cell uptake	47
		DNA	Base complementary pairing	FNA	Drug delivery	Enhanced delivery efficiency, responsive targeting	51
	MMP legumain HAase	Peptide	Hydrogen bond	Nanofiber, aggregate	Cell death, imaging, drug delivery	Signal amplification, extended retention time	60 and 66–68
		AuNPs	Click chemistry	Aggregate	Drug delivery	Extended retention time, improved drug utilization	69
		Polymer	Click chemistry	Aggregate	Drug delivery	Inhibition of the internalization of drug carriers, promotion of the interaction between drugs and plasma membrane	71
	Light, thermal	Peptide	Hydrophobic effect	Nanoparticles	Cell apoptosis	Extended retention time, destruction of the mitochondrial membrane	163
Wound microenvironment	H_2O_2	Polymer	Hydrogen bond	Polymer	Disease detection, bacteriostasis	Real-time naked eye monitoring	138
Bone space	pH	Polymer	Electrostatic interaction	Supramolecular hydrogel	Inhibition of absorption	Enhanced drug action	55
Blood vessel	Shear force	Polymer	Electrostatic interaction	Fiber network	Hemostasis	Compact structure	36
Liver	CMV promoter	siRNA	Base complementary pairing	Exosome	Drug delivery	Enhanced blood-brain barrier penetration	74
Cell membrane	ALP	Peptide	Hydrogen bond, hydrophobic effect	Aggregate, nanofiber, nanoparticles	Cell death, drug delivery, cell membrane phase separation	Endocytosis, apoptosis, prolonged retention time, increased drug permeability	82, 86–88 and 90
		Small molecules	Hydrogen bond	Aggregate, nanofiber	Imaging, drug delivery	Visualization, extended retention time, enhancement of cell uptake	29 and 92
	APS	Polymer and aptamer	Ligand–receptor interaction	Aggregate	Cell apoptosis	Regulation of cell fate	108
	CA IX	Peptide	Hydrophobic effect, Hydrogen bond	Aggregate	Cell membrane phase separation	Increased cell membrane penetration and drug utilization	84
	CD	DNA	RCA	Aggregate	Cancer treatment	Cancer targeting and value-added inhibition	111
		Peptide	Hydrogen bond	Fiber network, aggregate	Inhibition of angiogenesis and cancer metastasis, immunotherapy	Shielding effect of fiber network, T cell activation	106 and 107
		Polymer	Base complementary pairing	Nanocomposite	Cell apoptosis	Pre targeting, continuous administration	76
	Furin	Small molecules	Click chemistry	Nanoparticles	Drug delivery	High drug resistance, no cytotoxicity	101
		Peptide	Hydrogen bond	Fiber network	Inhibition of tumor growth	Decreased glucose uptake by tumor cells	98
	Thermal	Polymer	Hydrophobic effect	Aggregate	Imaging	Six-fold increase in fluorescence	167
	Toehold	DNA	Base complementary pairing	3D nano-prism	Bionics and delivery	Convenient for dynamic assembly	112
	$\alpha_V\beta_3$	Peptide	Hydrophobic effect, hydrogen bond	Nanoclusters, fiber network	Drug delivery, anti-angiogenesis	High drug resistance, shielding effect of fiber network	103 and 104
Intracellular	CES	Peptide	Hydrophobic effect, Hydrogen bond	Nanofiber	Drug delivery, cell death	Significant increase in drug resistance, affecting cell behavior	116 and 117
		Small molecules	π–π stacking	Nano brushes–Nanoparticles–Nanofiber	Drug delivery	Inhibition of metastasis and invasion of cancer cells	119
	XIAP	Peptide	Hydrogen bond	Superfiber network		Extended retention time	120

Table 2 (*continued*)

Trigger position	Stimulating response factor	Assembly material	Driving force	Assembly result	Applications	Advantages	Ref.
					Disease detection and treatment		
	Caspase, GSH, NTR	Peptide, small molecules	Hydrophobic effect, click chemistry	Aggregate, cyclic dimer, nanofiber, nanoparticles	Visual imaging, drug delivery	Enhanced photoacoustic signal, better magnetic resonance performance and mechanical strength, better biocompatibility	121, 122, 126 and 127
	ROS	Peptide and Polymer	Hydrophobic effect	Nanofiber	Cytotoxicity	Improved therapeutic effect	133
	Hypoxia	Small molecules	Click chemistry	Aggregate	Imaging	Amplified imaging signal	135
	pH	DNA	Base complementary pairing	Quadruplex	Drug delivery	Reversible on or off, intelligent response encapsulation or drug release	141
		Small molecules	π–π stacking, Hydrogen bond	Fiber	Cell death	Leading to lysosome rupture	144
	Light	Peptide	Hydrophobic effect	Nanodots	Imaging, photodynamic therapy	Extended of cycle	156
		Polymer	Polymerization	Nanoparticles	Imaging	Promoting actin polymerization, regulating cell fluidity	145
		DNA and small molecules	Base complementary pairing	G-quadruplex	Material manipulation, information collection	Significant signal amplification	149

factors in the lesion area and inducing *in situ* self-assembly of building blocks could be a feasible strategy to improve the cellular uptake of prodrugs. *In situ* self-assembled nanomaterials have been widely utilized in drug delivery, therapy, and imaging.[28,172–175] This review focuses on the self-assembly principles and biomedical applications related to tissue microenvironments, cell surfaces, intracellular stimulation, and exogenous stimulus-response. In particular, the review examines how the specific microenvironment of tumor tissue and cells and specific targets on the surface of tumor cells can induce the self-assembly of cancer lesions, enabling tumor-specific drug delivery and treatment. In general, self-assembly produces larger systems, which can be divided into nanoparticles, nanofibers, aggregates, networks, and more. Self-assembled molecules tend to change in size and shape, which offers several advantages, such as longer residence time, better endocytosis or penetration, signal amplification, higher drug delivery efficiency, visible fluorescence tracers, and more, all of which contribute to improved drug delivery and treatment *in vivo* (Table 2).

4. Challenges and prospectives

There are still many challenges that need to be overcome in the *in situ* construction of self-assembled nanosystems. This review proposes possible solutions to these challenges and discusses the expected development direction.

First, one of the major challenges is the complexity of the self-assembly process *in vivo*. The physiological environment is variable and unstable, leading to individual differences in organisms.[176] As such, designing molecular units that can accurately regulate the assembly process *in vivo* to improve the efficiency of drug delivery and the effectiveness of disease treatment remains a great challenge for researchers.[177–179] To address this, designing self-assembly molecules with multiple stimulus responses can improve the efficiency and effectiveness of self-assembly.[180] In addition, the coupling or driving forces between supramolecular self-assembly are mostly inferred from *in vitro* to *in vivo* experiments, and the real intermolecular interactions *in vivo* still need to be dynamically detected by developing more accurate characterization techniques or instruments to better understand *in vivo* assembly.[181] With the emergence of new materials and the increasing complexity of self-assembly structures, studying the effects of pathophysiological conditions on each interaction is crucial when designing a stimulus-response drug delivery system. Further basic research is needed to understand the interactions between selected materials and biological systems in terms of cell uptake, cytotoxicity, immunogenicity, *etc.*[182] In the research and development of new drugs, it is important to thoroughly study the mechanism and side effects of drugs before entering clinical research. Many drugs may quickly enter clinical research due to their excellent therapeutic effects in the experimental process. However, the failure of clinical trials or ineffective and counterproductive results in the human body may occur if the mechanism and side effects of drugs are not fully understood. Therefore, exploring methods

such as intermolecular interaction forces and molecular dynamics simulations, starting with theory and experimentally verifying it, can not only help lay the foundation but also save costs and reduce waste.[183,184]

Secondly, another challenge for assembled molecules is safety. Reversible self-assembly can degrade the assembled macromolecules into small molecules that can be more easily excreted or cleared by the organism. Consequently, it is imperative to develop biocompatible assembly monomers. Although materials capable of self-assembly mostly consist of exogenous substances, they are still less biocompatible than substances secreted by the body itself. Furthermore, small molecular prodrugs without carrier delivery lack multi-layer coated carriers, which can simplify the structure of nanoparticles. Nonetheless, their safety and stability require further investigation.

Thirdly, there are only a few reports on the controllable regulation of molecular size and reaction processes after *in situ* self-assembly *in vivo*. Due to the invisibility and uncontrollability of the *in situ* self-assembly process, researchers may encounter challenges in determining how far self-assembly has progressed and when to stop it. On one hand, previous studies have shown that the self-assembly formation time and growth rate can be controlled by adjusting the surface density of enzymes or modifying the local motifs of self-assembly precursors.[185] Additionally, adjusting the morphology and density of nanostructures can alter the mechanical properties of materials.[186] On the other hand, the introduction of luminescent motifs into self-assembly molecules can help visualize the process of *in situ* self-assembly, facilitating real-time monitoring.

Finally, it is crucial to investigate the critical aggregation concentration (CAC) required for self-assembly. The chemical complexity of the *in vivo* environment can interfere with the interactions between assembly motifs. Therefore, achieving *in situ* self-assembly at lesion sites *in vivo* necessitates higher concentrations of molecules, and the molecules themselves may have distinct roles compared to the practical application of self-assembled aggregates.[187] Combining exogenous stimuli with endogenous stimuli is a potent strategy to enhance the propensity for self-assembly. However, stimuli such as light and temperature can cause damage to cells or the human body.

As previously mentioned, the use of *in situ* stimulus-response self-assembly in drug delivery, fluorescence imaging, and precision therapy has seen significant progress. In addition to the challenges and possible solutions outlined above, understanding the self-assembly principles of biocompatible materials such as peptides, polymers, small molecules, nucleic acids, and other biocompatible materials is vital for further optimizing their properties, including interactions with living organisms and their long-term chemical and physical stability. The 2022 Nobel Prize in Chemistry was awarded to scientists in "click chemistry and biological orthogonal chemistry." Bioorthogonal reactions allow click chemistry to be performed within living cells without disrupting natural biochemical processes, and the *in situ* assembly and transformation of nanomaterials can be artificially controlled in space and time through bioorthogonal linkage and cleavage reactions.[188,189] The self-assembly process involves several click chemistry reactions, such as click-condensation reactions between cysteine (Cys) and CBT, and photoclick reaction coupling of maleimide and tetrazolium.[190,191] The number of investigations in this area is likely to increase significantly in the coming years.

The previous review showed that numerous enzymes are present in the tissue microenvironment, on the cell surface, or within cells. Accordingly, identifying the location of endogenous enzymes within living systems and achieving self-assembly of different parts is a potential way to treat cancer, which undoubtedly holds great promise for future development. In addition, the *in situ* self-assembly of therapeutic small molecular prodrugs within cellular environments has emerged as another practical strategy for developing multi-component targeted nano-drugs without drug resistance.[192] This approach can eliminate adverse reactions caused by carriers and achieve ultra-high drug loading, ensuring significant advantages in tumor drug resistance and increased drug payload. In the future, it may be possible to reduce systemic toxicity while maintaining anti-cancer efficacy, leading to clinical transformations in anti-tumor therapy.[193]

Author contributions

Conceptualization, Z. Y. and Z. L.; investigation, Z. Y. and Y. L.; writing – original draft preparation, Z. Y. and Y. L.; writing – review and editing, Z. L.; resources, L. Z., J. H., Y. D. and X. P.; project administration, Z. L.; funding acquisition, Z. L. All authors have read and agreed to the published version of the manuscript.

Conflicts of interest

There are no conflicts to declare.

Acknowledgements

This research was funded by the National Natural Science Foundation of China (32271464), the Hunan Provincial Natural Science Foundation for Distinguished Young Scholars (2022JJ10086), the Innovation-Driven Project of Central South University (2020CX048), the Natural Science Foundation of Changsha (kq2202131), the Postgraduate Innovation Project of Central South University (2021zzts0977, 2022zzts0980), and the Hunan Provincial Innovation Foundation for Postgraduate (CX20210340, CX20220372, QL20220035, QL20220036).

Notes and references

1 M. Monahan, M. Homer, S. Zhang, R. Zheng, C. L. Chen, J. De Yoreo and B. M. Cossairt, *ACS Nano*, 2022, **16**, 8095–8106.
2 M. Wen, N. Yu, S. Wu, M. Huang, P. Qiu, Q. Ren, M. Zhu and Z. Chen, *Bioact. Mater.*, 2022, **18**, 242–253.

3 Z. Lei, L. Ding, C. Yao, F. Mo, C. Li, Y. Huang, X. Yin, M. Li, J. Liu, Y. Zhang, C. Ling and Y. Wang, *Adv. Mater.*, 2019, **31**, e1807456.
4 C. F. Anderson, R. W. Chakroun, H. Su, R. E. Mitrut and H. Cui, *ACS Nano*, 2019, **13**, 12957–12968.
5 T. Ji and D. S. Kohane, *Nano Today*, 2019, **28**, 100765.
6 Z. Jiang, K. Li, Y. Luo, B. Chen, F. Meng, H. Yi, L. Zhang, H. Yang, W. Zhou, T. Cheng, H. Yi, Q. Yi, X. Wen, S. Hu, H. Liu and J. Chen, *Cancer Nanotechnol.*, 2022, **13**, 1–13.
7 Q. He, J. Chen, J. Yan, S. Cai, H. Xiong, Y. Liu, D. Peng, M. Mo and Z. Liu, *Asian J. Pharm. Sci.*, 2020, **15**, 416–448.
8 H. Nakatsuji, Y. Shioji, N. Hiraoka, Y. Okada, N. Kato, S. Shibata, I. Aoki and M. Matsusaki, *Mater. Horiz.*, 2021, **8**, 1216–1221.
9 J. M. Lehn, *Chem. Soc. Rev.*, 2007, **36**, 151–160.
10 L. L. Li, S. L. Qiao, W. J. Liu, Y. Ma, D. Wan, J. Pan and H. Wang, *Nat. Commun.*, 2017, **8**, 1276.
11 T. He, S. Qiao, C. Ma, Z. Peng, Z. Wu, C. Ma, L. Han, Q. Deng, T. Zhang, Y. Zhu and G. Pan, *J. Biomed. Mater. Res., Part B*, 2022, **110**, 2015–2027.
12 H. He, X. Lin, J. Guo, J. Wang and B. Xu, *ACS Nano*, 2020, **14**, 6947–6955.
13 L. J. Luo, X. M. Liu, X. Zhang, J. Liu, Y. Gao, T. Y. Sun and L. L. Li, *Nano Lett.*, 2022, **22**, 1694–1702.
14 Y. L. Luo, H. Y. Zhang, G. K. Li, Y. Y. Zhao, Y. Yang, R. X. Rong, X. L. Li and K. R. Wang, *ACS Macro Lett.*, 2022, **11**, 615–621.
15 J. Li, Y. Zhao, P. Zhou, X. Hu, D. Wang, S. M. King, S. E. Rogers, J. Wang, J. R. Lu and H. Xu, *Small*, 2020, **16**, e2003945.
16 D. H. Howe, K. J. Jenewein, J. L. Hart, M. L. Taheri and A. J. D. Magenau, *Polym. Chem.*, 2020, **11**, 298–303.
17 B. Becit and D. Zahn, *Microporous Mesoporous Mater.*, 2021, **320**, 111114.
18 L. Fan, Z. Zeng, R. Zhu, A. Liu, H. Che and M. Huo, *Chem. Mater.*, 2022, **34**, 6408–6419.
19 P. Wang, Y. Zou, Y. Li, Z. Qin, X. Liu and H. Zhang, *Food Hydrocolloids*, 2022, **131**, 107805.
20 H. Zhang, K. Liu, Y. Gong, W. Zhu, J. Zhu, F. Pan, Y. Chao, Z. Xiao, Y. Liu, X. Wang, Z. Liu, Y. Yang and Q. Chen, *Biomaterials*, 2022, **287**, 121673.
21 B. Lindman, B. Medronho, L. Alves, M. Norgren and L. Nordenskiold, *Q. Rev. Biophys.*, 2021, **54**, e3.
22 K. Liu, X.-Q. Zha, Q.-M. Li, L.-H. Pan and J.-P. Luo, *Food Hydrocolloids*, 2021, **118**, 106807.
23 J. T. Sharick, A. J. Atieh, K. J. Gooch and J. L. Leight, *J. Biomed. Mater. Res., Part A*, 2022, **111**, 389–403.
24 G. B. Qi, Y. J. Gao, L. Wang and H. Wang, *Adv. Mater.*, 2018, **30**, e1703444.
25 N. Liu, L. Zhu, Z. Li, W. Liu, M. Sun and Z. Zhou, *Biomater. Sci.*, 2021, **9**, 5427–5436.
26 Y. Zhang, Y. Yu and J. Gao, *Front. Chem.*, 2022, **10**, 815551.
27 S. H. Kwon, D. Lee, H. Kim, Y. J. Jung, H. Koo and Y. B. Lim, *Mater. Today Bio*, 2022, **16**, 100337.
28 J. Shen, K. Shao, W. Zhang and Y. He, *ACS Macro Lett.*, 2021, **10**, 702–707.
29 Q. Wang, M. Xiao, D. Wang, X. Hou, J. Gao, J. Liu and J. Liu, *Adv. Funct. Mater.*, 2021, **31**, 2101826.
30 K. He, J. Zhu, L. Gong, Y. Tan, H. Chen, H. Liang, B. Huang and J. Liu, *Nano Res.*, 2020, **14**, 1087–1094.
31 F. Semcheddine, N. El Islem Guissi, W. Liu, Tayyaba, L. Gang, H. Jiang and X. Wang, *Mater. Horiz.*, 2021, **8**, 2771–2784.
32 M. Shekhirev, E. Sutter and P. Sutter, *Adv. Funct. Mater.*, 2019, **29**, 1806924.
33 D. Barkley, R. Moncada, M. Pour, D. A. Liberman, I. Dryg, G. Werba, W. Wang, M. Baron, A. Rao, B. Xia, G. S. Franca, A. Weil, D. F. Delair, C. Hajdu, A. W. Lund, I. Osman and I. Yanai, *Nat. Genet.*, 2022, **54**, 1192–1201.
34 S. Srinivasan, T. Kryza, J. Batra and J. Clements, *Nat. Rev. Cancer*, 2022, **22**, 223–238.
35 S. Yamamoto, K. Nishimura, K. Morita, S. Kanemitsu, Y. Nishida, T. Morimoto, T. Aoi, A. Tamura and T. Maruyama, *Biomacromolecules*, 2021, **22**, 2524–2531.
36 C. He, T. Ye, W. Teng, Z. Fang, W. S. Ruan, G. Liu, H. Chen, J. Sun, L. Hui, F. Sheng, D. Pan, C. Yang, Y. Zheng, M. B. Luo, K. Yao and B. Wang, *ACS Nano*, 2019, **13**, 1910–1922.
37 M. W. Parker, M. Bell, M. Mir, J. A. Kao, X. Darzacq, M. R. Botchan and J. M. Berger, *eLife*, 2019, **8**, e48562.
38 M. Wang, J. Li, X. Li, H. Mu, X. Zhang, Y. Shi, Y. Chu, A. Wang, Z. Wu and K. Sun, *J. Controlled Release*, 2016, **232**, 161–174.
39 N. Rohani, L. Hao, M. S. Alexis, B. A. Joughin, K. Krismer, M. N. Moufarrej, A. R. Soltis, D. A. Lauffenburger, M. B. Yaffe, C. B. Burge, S. N. Bhatia and F. B. Gertler, *Cancer Res.*, 2019, **79**, 1952–1966.
40 Z. Cheng, Y. Cheng, Q. Chen, M. Li, J. Wang, H. Liu, M. Li, Y. Ning, Z. Yu, Y. Wang and H. Wang, *Nano Today*, 2020, **33**, 100878.
41 M. Li, Y. Ning, J. Chen, X. Duan, N. Song, D. Ding, X. Su and Z. Yu, *Nano Lett.*, 2019, **19**, 7965–7976.
42 B. Sun, R. Chang, S. Cao, C. Yuan, L. Zhao, H. Yang, J. Li, X. Yan and J. C. M. van Hest, *Angew. Chem., Int. Ed.*, 2020, **59**, 20582–20588.
43 X. Wang, M. Li, Y. Hou, Y. Li, X. Yao, C. Xue, Y. Fei, Y. Xiang, K. Cai, Y. Zhao and Z. Luo, *Adv. Funct. Mater.*, 2020, **30**, 2000229.
44 M. Li, Z. Wang, X. Liu, N. Song, Y. Song, X. Shi, J. Liu, J. Liu and Z. Yu, *J. Controlled Release*, 2021, **340**, 35–47.
45 Y. Song, Q. Su, H. Song, X. Shi, M. Li, N. Song, S. Lou, W. Wang and Z. Yu, *ACS Appl. Mater. Interfaces*, 2021, **13**, 49737–49753.
46 A. Awaad, H. Takemoto, M. Iizuka, K. Ogi, Y. Mochida, A. H. Ranneh, M. Toyoda, M. Matsui, T. Nomoto, Y. Honda, K. Hayashi, K. Tomoda, T. Ohtake, Y. Miura and N. Nishiyama, *J. Controlled Release*, 2022, **346**, 392–404.
47 C. Liu, Q. Liu, L. Chen, M. Li, J. Yin, X. Zhu and D. Chen, *Adv. Healthcare Mater.*, 2020, **9**, e2000899.
48 M. Nishino, I. Matsuzaki, F. Y. Musangile, Y. Takahashi, Y. Iwahashi, K. Warigaya, Y. Kinoshita, F. Kojima and S. I. Murata, *PLoS One*, 2020, **15**, e0236373.

49 T. Ma, R. Chen, N. Lv, Y. Chen, H. Qin, H. Jiang and J. Zhu, *Small*, 2022, **18**, e2106291.
50 X. Sun, J. Zhang, C. Yang, Z. Huang, M. Shi, S. Pan, H. Hu, M. Qiao, D. Chen and X. Zhao, *ACS Appl. Mater. Interfaces*, 2019, **11**, 11865–11875.
51 P. Peng, Q. Wang, Y. Du, H. Wang, L. Shi and T. Li, *Anal. Chem.*, 2020, **92**, 9273–9280.
52 P. Peng, Y. Du, J. Zheng, H. Wang and T. Li, *Angew. Chem., Int. Ed.*, 2019, **58**, 1648–1653.
53 J. Zheng, Q. Wang, L. Shi, L. Shi and T. Li, *Anal. Chem.*, 2022, **94**, 9097–9105.
54 Y. Feng, Q. Liu, M. Chen, X. Zhao, L. Wang, L. Liu and X. Chen, *Chem. Commun.*, 2021, **57**, 10935–10938.
55 A. Tang, Y. Qian, S. Liu, W. Wang, B. Xu, A. Qin and G. Liang, *Nanoscale*, 2016, **8**, 10570–10575.
56 G. Di Pompo, M. Cortini, N. Baldini and S. Avnet, *Cancers*, 2021, **13**, 1–21.
57 C. Zhao, N. T. Qazvini, M. Sadati, Z. Zeng, S. Huang, A. L. De La Lastra, L. Zhang, Y. Feng, W. Liu, B. Huang, B. Zhang, Z. Dai, Y. Shen, X. Wang, W. Luo, B. Liu, Y. Lei, Z. Ye, L. Zhao, D. Cao, L. Yang, X. Chen, A. Athiviraham, M. J. Lee, J. M. Wolf, R. R. Reid, M. Tirrell, W. Huang, J. J. de Pablo and T. C. He, *ACS Appl. Mater. Interfaces*, 2019, **11**, 8749–8762.
58 F. Zhang, Q. Hu, Y. Wei, W. Meng, R. Wang, J. Liu, Y. Nie, R. Luo, Y. Wang and B. Shen, *Chem. Eng. J.*, 2022, **435**, 134802.
59 Q. Zhang, M. He, X. Zhang, H. Yu, J. Liu, Y. Guo, J. Zhang, X. Ren, H. Wang and Y. Zhao, *Adv. Funct. Mater.*, 2022, **32**, 2112251.
60 A. Tanaka, Y. Fukuoka, Y. Morimoto, T. Honjo, D. Koda, M. Goto and T. Maruyama, *J. Am. Chem. Soc.*, 2015, **137**, 770–775.
61 D. Bacinello, E. Garanger, D. Taton, K. C. Tam and S. Lecommandoux, *Biomacromolecules*, 2014, **15**, 1882–1888.
62 L. Yang, J. Tang, H. Yin, J. Yang, B. Xu, Y. Liu, Z. Hu, B. Yu, F. Xia and G. Zou, *ACS Biomater. Sci. Eng.*, 2022, **8**, 880–892.
63 X. Hu, P. Yang, J. He, R. Liang, D. Niu, H. Wang and Y. Li, *J. Mater. Chem. B*, 2017, **5**, 5931–5936.
64 L. Wang, H. Li, L. Shi, L. Li, F. Jia, T. Gao and G. Li, *Biosens. Bioelectron.*, 2022, **195**, 113671.
65 S. Z. Lu, X. Y. Guo, M. S. Zou, Z. Q. Zheng, Y. C. Li, X. D. Li, L. L. Li and H. Wang, *Adv. Healthcare Mater.*, 2020, **9**, e1901229.
66 X. Jiang, X. Fan, W. Xu, C. Zhao, H. Wu, R. Zhang and G. Wu, *J. Controlled Release*, 2019, **316**, 196–207.
67 H. W. An, D. Hou, R. Zheng, M. D. Wang, X. Z. Zeng, W. Y. Xiao, T. D. Yan, J. Q. Wang, C. H. Zhao, L. M. Cheng, J. M. Zhang, L. Wang, Z. Q. Wang, H. Wang and W. Xu, *ACS Nano*, 2020, **14**, 927–936.
68 D. Y. Hou, M. D. Wang, X. J. Hu, Z. J. Wang, N. Y. Zhang, G. T. Lv, J. Q. Wang, X. H. Wu, L. Wang, H. Wang and W. Xu, *Bioact. Mater.*, 2022, **14**, 110–119.
69 S. Ruan, C. Hu, X. Tang, X. Cun, W. Xiao, K. Shi, Q. He and H. Gao, *ACS Nano*, 2016, **10**, 10086–10098.
70 S. Ruan, R. Xie, L. Qin, M. Yu, W. Xiao, C. Hu, W. Yu, Z. Qian, L. Ouyang, Q. He and H. Gao, *Nano Lett.*, 2019, **19**, 8318–8332.
71 Q. Hu, W. Sun, Y. Lu, H. N. Bomba, Y. Ye, T. Jiang, A. J. Isaacson and Z. Gu, *Nano Lett.*, 2016, **16**, 1118–1126.
72 Y. B. Johari, J. M. Scarrott, T. H. Pohle, P. Liu, A. Mayer, A. J. Brown and D. C. James, *Biotechnol. J.*, 2022, **17**, e2200062.
73 Z. Fu, X. Zhang, X. Zhou, U. Ur-Rehman, M. Yu, H. Liang, H. Guo, X. Guo, Y. Kong, Y. Su, Y. Ye, X. Hu, W. Cheng, J. Wu, Y. Wang, Y. Gu, S. F. Lu, D. Wu, K. Zen, J. Li, C. Yan, C. Y. Zhang and X. Chen, *Cell Res.*, 2021, **31**, 631–648.
74 L. Zhang, T. Wu, Y. Shan, G. Li, X. Ni, X. Chen, X. Hu, L. Lin, Y. Li, Y. Guan, J. Gao, D. Chen, Y. Zhang, Z. Pei and X. Chen, *Brain*, 2021, **144**, 3421–3435.
75 S. Carapezzi, G. Boschetto and A. Todri-Sanial, *Nanoscale Adv.*, 2022, **4**, 4131–4137.
76 T. W. Chu, J. Y. Yang, R. Zhang, M. Sima and J. Kopeček, *ACS Nano*, 2014, **8**, 719–730.
77 R. Das, R. F. Landis, G. Y. Tonga, R. Cao-Milan, D. C. Luther and V. M. Rotello, *ACS Nano*, 2019, **13**, 229–235.
78 X. Yang, L. Yang, D. Yang, M. Li and P. Wang, *Nano Lett.*, 2022, **22**, 3410–3416.
79 X. Y. Zhang, C. Liu, P. S. Fan, X. H. Zhang, D. Y. Hou, J. Q. Wang, H. Yang, H. Wang and Z. Y. Qiao, *J. Mater. Chem. B*, 2022, **10**, 3624–3636.
80 E. Du, X. Hu, G. Li, S. Zhang, D. Mang, S. Roy, T. Sasaki and Y. Zhang, *Langmuir*, 2019, **35**, 7376–7382.
81 Y. Su, X. Chen, H. Wang, L. Sun, Y. Xu and D. Li, *Chem. Sci.*, 2022, **13**, 6303–6308.
82 R. C. Guo, X. H. Zhang, P. S. Fan, B. L. Song, Z. X. Li, Z. Y. Duan, Z. Y. Qiao and H. Wang, *Angew. Chem., Int. Ed.*, 2021, **60**, 25128–25134.
83 J. Li, K. Shi, Z. F. Sabet, W. Fu, H. Zhou, S. Xu, T. Liu, M. You, M. Cao, M. Xu, X. Cui, B. Hu, Y. Liu and C. Chen, *Sci. Adv.*, 2019, **5**, 1–15.
84 Z. Wang, H. W. An, D. Hou, M. Wang, X. Zeng, R. Zheng, L. Wang, K. Wang, H. Wang and W. Xu, *Adv. Mater.*, 2019, **31**, e1807175.
85 Z. G. Yang, C. Ge, J. Liu, Y. Chong, Z. Gu, C. A. Jimenez-Cruz, Z. Chai and R. Zhou, *Nanoscale*, 2015, **7**, 18725–18737.
86 W. Tang, Z. Zhao, Y. Chong, C. Wu, Q. Liu, J. Yang, R. Zhou, Z. X. Lian and G. Liang, *ACS Nano*, 2018, **12**, 9966–9973.
87 W. Tang, J. Yang, Z. Zhao, Z. Lian and G. Liang, *Nanoscale*, 2017, **9**, 17717–17721.
88 L. R. Hart, S. M. Mitchell, P. A. McCallum, R. E. Daso and I. A. Banerjee, *Soft Mater.*, 2021, **20**, 109–128.
89 H. He, J. Guo, J. Xu, J. Wang, S. Liu and B. Xu, *Nano Lett.*, 2021, **21**, 4078–4085.
90 R. A. Pires, Y. M. Abul-Haija, D. S. Costa, R. Novoa-Carballal, R. L. Reis, R. V. Ulijn and I. Pashkuleva, *J. Am. Chem. Soc.*, 2015, **137**, 576–579.
91 H. Wang, Z. Feng, Y. Wang, R. Zhou, Z. Yang and B. Xu, *J. Am. Chem. Soc.*, 2016, **138**, 16046–16055.
92 M. Zhang, C. Wang, C. Yang, H. Wu, H. Xu and G. Liang, *Anal. Chem.*, 2021, **93**, 5665–5669.

93 Y. Li, R. Xie, X. Pang, Z. Zhou, H. Xu, B. Gu, C. Wu, H. Li and Y. Zhang, *Talanta*, 2019, **205**, 120143.
94 L. Zhang, Y. Li, G. Mu, L. Yang, C. Ren, Z. Wang, Q. Guo, J. Liu and C. Yang, *Anal. Chem.*, 2022, **94**, 2236–2243.
95 R. Yan, Y. Hu, F. Liu, S. Wei, D. Fang, A. J. Shuhendler, H. Liu, H. Y. Chen and D. Ye, *J. Am. Chem. Soc.*, 2019, **141**, 10331–10341.
96 L. Huang, X. Cao, T. Gao, B. Feng, X. Huang, R. Song, T. Du, S. Wen, X. Feng and W. Zeng, *Talanta*, 2021, **225**, 121950.
97 X. Li, C. Cao, P. Wei, M. Xu, Z. Liu, L. Liu, Y. Zhong, R. Li, Y. Zhou and T. Yi, *ACS Appl. Mater. Interfaces*, 2019, **11**, 12327–12334.
98 G. Kwek, S. Lingesh, S. Z. Chowdhury and B. Xing, *Chem. Commun.*, 2022, **58**, 1350–1353.
99 Y. Yuan, P. Raj, J. Zhang, S. Siddhanta, I. Barman and J. W. M. Bulte, *Angew. Chem., Int. Ed.*, 2021, **60**, 3923–3927.
100 J. Dai, M. Chen, D. Xu, H. Li, Y. Qiao, X. Ke and T. Ci, *Nanomedicine*, 2021, **16**, 355–372.
101 Y. Yuan, L. Wang, W. Du, Z. Ding, J. Zhang, T. Han, L. An, H. Zhang and G. Liang, *Angew. Chem., Int. Ed.*, 2015, **127**, 9836–9840.
102 M. D. Wang, D. Y. Hou, G. T. Lv, R. X. Li, X. J. Hu, Z. J. Wang, N. Y. Zhang, L. Yi, W. H. Xu and H. Wang, *Biomaterials*, 2021, **278**, 121139.
103 L. B. Case and C. M. Waterman, *Nat. Cell Biol.*, 2015, **17**, 955–963.
104 K. Zhang, H. Zhang, Y. H. Gao, J. Q. Wang, Y. Li, H. Cao, Y. Hu and L. Wang, *ACS Nano*, 2021, **15**, 13065–13076.
105 S. Luo, J. Feng, L. Xiao, L. Guo, L. Deng, Z. Du, Y. Xue, X. Song, X. Sun, Z. Zhang, Y. Fu and T. Gong, *Biomaterials*, 2020, **249**, 120055.
106 M. D. Wang, G. T. Lv, H. W. An, N. Y. Zhang and H. Wang, *Angew. Chem., Int. Ed.*, 2022, **61**, e202113649.
107 L. Wang, Y. Lv, C. Li, G. Yang, B. Fu, Q. Peng, L. Jian, D. Hou, J. Wang, C. Zhao, P. Yang, K. Zhang, L. Wang, Z. Wang, H. Wang and W. Xu, *Small*, 2020, **16**, 2004548.
108 J. Qi, W. Li, X. Xu, F. Jin, D. Liu, Y. Du, J. Wang, X. Ying, J. You, Y. Du and J. Ji, *Chem. Sci.*, 2020, **11**, 4221–4225.
109 L. Li, J. Wang, Y. Li, D. C. Radford, J. Yang and J. Kopecek, *ACS Nano*, 2019, **13**, 11422–11432.
110 M. Y. Lv, W. Y. Xiao, Y. P. Zhang, L. L. Jin, Z. H. Li, Z. Lei, D. B. Cheng and S. D. Jin, *Colloids Surf., B*, 2022, **217**, 112655.
111 J. Wang, Z. Zhang, R. Zhang, H. Du, T. Zhou and F. Wang, *Langmuir*, 2022, **38**, 11778–11786.
112 R. Peng, H. Wang, Y. Lyu, L. Xu, H. Liu, H. Kuai, Q. Liu and W. Tan, *J. Am. Chem. Soc.*, 2017, **139**, 12410–12413.
113 H. He, Y. Lu, J. Qi, Q. Zhu, Z. Chen and W. Wu, *Acta Pharm. Sin. B*, 2019, **9**, 36–48.
114 K. N. Baumann, L. Piantanida, J. Garcia-Nafria, D. Sobota, K. Voitchovsky, T. P. J. Knowles and S. Hernandez-Ainsa, *ACS Nano*, 2020, **14**, 2316–2323.
115 Z. Feng, H. Wang, X. Chen and B. Xu, *J. Am. Chem. Soc.*, 2017, **139**, 15377–15384.
116 Z. M. Yang, K. M. Xu, Z. F. Guo, Z. H. Guo and B. Xu, *Adv. Mater.*, 2007, **19**, 3152–3156.
117 Y. Gao, Y. Kuang, X. Du, J. Zhou, P. Chandran, F. Horkay and B. Xu, *Langmuir*, 2013, **29**, 15191–15200.
118 Z. Wang, Z. Xiong, W. Liu, Q. Zhu, X. Zhang, Y. Ding, C. Huang, H. Feng, K. Zhang, E. Zhu and Z. Qian, *Anal. Chem.*, 2022, **94**, 5406–5414.
119 G. Gao, Y. Jiang, W. Zhan, X. Liu, R. Tang, X. Sun, Y. Deng, L. Xu and G. Liang, *J. Am. Chem. Soc.*, 2022, **144**, 11897–11910.
120 H. W. An, L. L. Li, Y. Wang, Z. Wang, D. Hou, Y. X. Lin, S. L. Qiao, M. D. Wang, C. Yang, Y. Cong, Y. Ma, X. X. Zhao, Q. Cai, W. T. Chen, C. Q. Lu, W. Xu, H. Wang and Y. Zhao, *Nat. Commun.*, 2019, **10**, 4861.
121 Y. Yuan, Z. Ding, J. Qian, J. Zhang, J. Xu, X. Dong, T. Han, S. Ge, Y. Luo, Y. Wang, K. Zhong and G. Liang, *Nano Lett.*, 2016, **16**, 2686–2691.
122 Q. Cai, Y. Fei, L. Hu, Z. Huang, L. L. Li and H. Wang, *Nano Lett.*, 2018, **18**, 6229–6236.
123 Y. Bai, Y. Pan, N. An, H. Zhang, C. Wang, W. Tian and T. Huang, *Chin. Chem. Lett.*, 2023, **34**, 107552.
124 Z. Zheng, P. Chen, M. Xie, C. Wu and Y. Luo, *J. Am. Chem. Soc.*, 2016, **138**, 11128–11131.
125 K. Teng, X. Luan, Q. An, Y. Zhao, X. Hu, S. Zhang, J. Zhuang, X. Li, L. Lu and Y. Zhang, *ChemistrySelect*, 2020, **5**, 5781–5787.
126 M. M. Zhang, Y. Guan, Z. Dang, P. G. Zhang, C. Zheng, L. Chen, W. Kuang, C. C. Wang and G. L. Liang, *Sci. Adv.*, 2020, **6**, 1–6.
127 S. Liu, A. Tang, M. Xie, Y. Zhao, J. Jiang and G. Liang, *Angew. Chem., Int. Ed.*, 2015, **127**, 3710–3713.
128 K. Chen, Q. Lin, L. Wang, Z. Zhuang, Y. Zhang, D. Huang and H. Wang, *ACS Appl. Mater. Interfaces*, 2021, **13**, 9748–9761.
129 A. Chalard, M. Mauduit, S. Souleille, P. Joseph, L. Malaquin and J. Fitremann, *Addit. Manuf.*, 2020, **33**, 101162.
130 L. Li, L. Shi, J. Jia, O. Eltayeb, W. Lu, Y. Tang, C. Dong and S. Shuang, *ACS Appl. Mater. Interfaces*, 2020, **12**, 18250–18257.
131 H. He, Q. Yang, H. Li, S. Meng, Z. Xu, X. Chen, Z. Sun, B. Jiang and C. Li, *Mikrochim. Acta*, 2021, **188**, 141.
132 L. Wu, Y. Shi, Z. Ni, T. Yu and Z. Chen, *Mol. Pharmaceutics*, 2022, **19**, 35–50.
133 D. B. Cheng, X. H. Zhang, Y. J. Gao, L. Ji, D. Hou, Z. Wang, W. Xu, Z. Y. Qiao and H. Wang, *J. Am. Chem. Soc.*, 2019, **141**, 7235–7239.
134 S. Kim, B. Jana, E. M. Go, J. E. Lee, S. Jin, E. K. An, J. Hwang, Y. Sim, S. Son, D. Kim, C. Kim, J. O. Jin, S. K. Kwak and J. H. Ryu, *ACS Nano*, 2021, **15**, 14492–14508.
135 H. Zhou, M. Guo, J. Li, F. Qin, Y. Wang, T. Liu, J. Liu, Z. F. Sabet, Y. Wang, Y. Liu, Q. Huo and C. Chen, *J. Am. Chem. Soc.*, 2021, **143**, 1846–1853.
136 X. Yang, B. Wu, J. Zhou, H. Lu, H. Zhang, F. Huang and H. Wang, *Nano Lett.*, 2022, **22**, 7588–7596.
137 S. Wang, H. Zheng, L. Zhou, F. Cheng, Z. Liu, H. Zhang, L. Wang and Q. Zhang, *Nano Lett.*, 2020, **20**, 5149–5158.
138 A. Wang, G. Fan, H. Qi, H. Li, C. Pang, Z. Zhu, S. Ji, H. Liang, B. P. Jiang and X. C. Shen, *Biomaterials*, 2022, **289**, 121798.
139 C. Sun, Z. Wang, K. Yang, L. Yue, Q. Cheng, Y. L. Ma, S. Lu, G. Chen and R. Wang, *Small*, 2021, **17**, e2101139.

140 Q. Xia, S. Feng, J. Hong and G. Feng, *Talanta*, 2021, **228**, 122184.
141 C. Wang, Y. Du, Q. Wu, S. Xuan, J. Zhou, J. Song, F. Shao and H. Duan, *Chem. Commun.*, 2013, **49**, 5739–5741.
142 S. Son, J. Nam, J. Kim, S. Kim and W. J. Kim, *J. Am. Chem. Soc.*, 2014, **8**, 5574–5584.
143 S. H. Kim, K. R. Kim, D. R. Ahn, J. E. Lee, E. G. Yang and S. Y. Kim, *ACS Nano*, 2017, **11**, 9352–9359.
144 C. Keum, J. Hong, D. Kim, S. Y. Lee and H. Kim, *ACS Appl. Mater. Interfaces*, 2021, **13**, 14866–14874.
145 J. Geng, W. Li, Y. Zhang, N. Thottappillil, J. Clavadetscher, A. Lilienkampf and M. Bradley, *Nat. Chem.*, 2019, **11**, 578–586.
146 L. Chen, M. Xu, J. Hu and Q. Yan, *Macromolecules*, 2017, **50**, 4276–4280.
147 M. A. Uddin, H. Yu, L. Wang, B. U. Amin, S. Mehmood, R. Liang, F. Haq, J. Hu and J. Xu, *ACS Appl. Mater. Interfaces*, 2021, **13**, 61693–61706.
148 J. Ryssy, A. K. Natarajan, J. Wang, A. J. Lehtonen, M. K. Nguyen, R. Klajn and A. Kuzyk, *Angew. Chem., Int. Ed.*, 2021, **60**, 5859–5863.
149 Q. Jiang, Q. Liu, Y. Shi, Z. G. Wang, P. Zhan, J. Liu, C. Liu, H. Wang, X. Shi, L. Zhang, J. Sun, B. Ding and M. Liu, *Nano Lett.*, 2017, **17**, 7125–7130.
150 L. Xu, F. Mou, H. Gong, M. Luo and J. Guan, *Chem. Soc. Rev.*, 2017, **46**, 6905–6926.
151 P. Li, G. Xie, P. Liu, X. Y. Kong, Y. Song, L. Wen and L. Jiang, *J. Am. Chem. Soc.*, 2018, **140**, 16048–16052.
152 Q. Ren, X. Tang, Y. Lu, Q. Li, Z. Liao, S. Jiang, H. Zhang, Z. Xu and L. Luo, *Asian J. Pharm. Sci.*, 2022, **17**, 596–609.
153 X. Fan, T. Yue, A. Liu, X. Xie, W. Fang, Y. Wei, H. Zheng, H. Zheng, M. Zhou, J. Piao and F. Li, *Asian J. Pharm. Sci.*, 2022, **17**, 713–727.
154 W. Zeng, Z. Li, H. Chen, X. Zeng and L. Mei, *Cell Rep. Phys. Sci.*, 2022, **3**, 100898.
155 X. Zhao, K. Zhang, Y. Wang, W. Jiang, H. Cheng, Q. Wang, T. Xiang, Z. Zhang, J. Liu and J. Shi, *Adv. Funct. Mater.*, 2022, **32**, 2108883.
156 Y. Jia, J. Li, J. Chen, P. Hu, L. Jiang, X. Chen, M. Huang, Z. Chen and P. Xu, *ACS Appl. Mater. Interfaces*, 2018, **10**, 15369–15380.
157 N. Y. Zhang, X. J. Hu, H. W. An, J. X. Liang and H. Wang, *Biomaterials*, 2022, **287**, 121655.
158 M. Hou, W. Chen, J. Zhao, D. Dai, M. Yang and C. Yi, *Chin. Chem. Lett.*, 2022, **33**, 4101–4106.
159 C. Yang, F. Hu, X. Zhang, C. Ren, F. Huang, J. Liu, Y. Zhang, L. Yang, Y. Gao, B. Liu and J. Liu, *Biomaterials*, 2020, **244**, 119972.
160 Y. Li, D. Hu, Z. Sheng, T. Min, M. Zha, J. S. Ni, H. Zheng and K. Li, *Biomaterials*, 2021, **264**, 120365.
161 S. Luo, X. Luo, X. Wang, L. Li, H. Liu, B. Mo, H. Gan, W. Sun, L. Wang, H. Liang and S. Yu, *Small*, 2022, **18**, e2201298.
162 D. Wu, S. Xu, X. Zhang, Y. Li, W. Zhang, Q. Yan, Q. Yang, F. Guo and G. Yang, *ACS Appl. Mater. Interfaces*, 2021, **13**, 16036–16047.
163 F. H. Liu, Y. Cong, G. B. Qi, L. Ji, Z. Y. Qiao and H. Wang, *Nano Lett.*, 2018, **18**, 6577–6584.
164 X. Ma, X. Chen, Z. Yi, Z. Deng, W. Su, G. Chen, L. Ma, Y. Ran, Q. Tong and X. Li, *ACS Appl. Mater. Interfaces*, 2022, **14**, 26431–26442.
165 J. He, J. Cao, Y. Chen, L. Zhang and J. Tan, *ACS Macro Lett.*, 2020, **9**, 533–539.
166 X. Gong, G. Qi, Y. Li, K. Zhang, Y. Gao, D. Wang, H. Cao, Z. Yang and L. Wang, *J. Mater. Chem. B*, 2022, **10**, 3886–3894.
167 S. L. Qiao, Y. Wang, Y. X. Lin, H. W. An, Y. Ma, L. L. Li, L. Wang and H. Wang, *ACS Appl. Mater. Interfaces*, 2016, **8**, 17016–17022.
168 H. Tao, E. Galati and E. Kumacheva, *Macromolecules*, 2018, **51**, 6021–6027.
169 S. Wang, W. He, C. Xiao, Y. Tao and X. Wang, *Biomacromolecules*, 2019, **20**, 1655–1666.
170 V. Del Genio, A. Falanga, E. Allard-Vannier, K. Herve-Aubert, M. Leone, R. Bellavita, R. Uzbekov, I. Chourpa and S. Galdiero, *Pharmaceutics*, 2022, **14**, 1544.
171 H. Q. Peng, B. Liu, P. Wei, P. Zhang, H. Zhang, J. Zhang, K. Li, Y. Li, Y. Cheng, J. W. Y. Lam, W. Zhang, C. S. Lee and B. Z. Tang, *ACS Nano*, 2019, **13**, 839–846.
172 L. Lei, M. Li, S. Wu, Z. Xu, P. Geng, Y. Tian, Y. Fu and W. Zhang, *Anal. Chem.*, 2020, **92**, 5838–5845.
173 Y. Hu, J. Zhang, Y. Miao, X. Wen, J. Wang, Y. Sun, Y. Chen, J. Lin, L. Qiu, K. Guo, H. Y. Chen and D. Ye, *Angew. Chem., Int. Ed.*, 2021, **60**, 18082–18093.
174 J. Wang, J. Li, M. Li, K. Ma, D. Wang, L. Su, X. Zhang and B. Z. Tang, *J. Am. Chem. Soc.*, 2022, **144**, 14388–14395.
175 M. Wang, Z. Guo, J. Zeng, L. Liu, Y. Wang, J. Wang, H. Lu, H. Zhang, H. Jiang and X. Wang, *Chin. Chem. Lett.*, 2023, **34**, 107651.
176 M. Mamuti, R. Zheng, H.-W. An and H. Wang, *Nano Today*, 2021, **36**, 101036.
177 A. R. Willmer, J. Nie, M. V. George De la Rosa, W. Wen, S. Dunne and G. R. Rosania, *J. Controlled Release*, 2022, **347**, 620–631.
178 J. Yang, D. Zhao, D. Yao, Y. Wang and H. Li, *Chem. Eng. J.*, 2021, **426**, 131595.
179 H. Wang, M. Monroe, F. Leslie, C. Flexner and H. Cui, *Trends Pharmacol. Sci.*, 2022, **43**, 510–521.
180 S. Chagri, D. Y. W. Ng and T. Weil, *Nat. Rev. Chem.*, 2022, **6**, 320–338.
181 X. Liang, Y. Zhang, J. Zhou, Z. Bu, J. Liu and K. Zhang, *Coord. Chem. Rev.*, 2022, **473**, 214824.
182 A. Sarode, A. Annapragada, J. Guo and S. Mitragotri, *Biomaterials*, 2020, **242**, 119929.
183 M. C. Mañas-Torres, C. Gila-Vilchez, J. A. González-Vera, F. Conejero-Lara, V. Blanco, J. M. Cuerva, M. T. Lopez-Lopez, A. Orte and L. Álvarez de Cienfuegos, *Mater. Chem. Front.*, 2021, **5**, 5452–5462.
184 Q. Dong, M. Wang, A. Wang, C. Yu, S. Bai, J. Yin and Q. You, *Biomater. Sci.*, 2022, **10**, 1470–1475.
185 T. Miki, K. Kajiwara, S. Nakayama, M. Hashimoto and H. Mihara, *ACS Synth. Biol.*, 2022, **11**, 2144–2153.

186 C. Muller, A. Ontani, A. Bigo-Simon, P. Schaaf and L. Jierry, *Adv. Colloid Interface Sci.*, 2022, **304**, 102660.
187 M. T. Jeena, L. Palanikumar, E. M. Go, I. Kim, M. G. Kang, S. Lee, S. Park, H. Choi, C. Kim, S. M. Jin, S. C. Bae, H. W. Rhee, E. Lee, S. K. Kwak and J. H. Ryu, *Nat. Commun.*, 2017, **8**, 26.
188 J. Lin, D. Gao, S. Wang, G. Lv, X. Wang, C. Lu, Y. Peng and L. Qiu, *J. Am. Chem. Soc.*, 2022, **144**, 7667–7675.
189 X. Zhang, R. F. Landis, P. Keshri, R. Cao-Milan, D. C. Luther, S. Gopalakrishnan, Y. Liu, R. Huang, G. Li, M. Malassine, I. Uddin, B. Rondon and V. M. Rotello, *Adv. Healthcare Mater.*, 2021, **10**, e2001627.
190 L. Chen, X. Li and Q. Yan, *Macromolecules*, 2021, **54**, 5077–5086.
191 D. Ji, S. Y. Yoon, G. Kim, Y. Reo, S. H. Lee, H. G. Girma, S. Jeon, S. H. Jung, D. H. Hwang, J. Y. Kim, B. Lim and Y. Y. Noh, *Chem. Eng. J.*, 2023, **452**, 139500.
192 S. Zhang and Y. Zhang, *ACS Appl. Mater. Interfaces*, 2020, **12**, 41105–41112.
193 G. Li, B. Sun, Y. Li, C. Luo, Z. He and J. Sun, *Small*, 2021, **17**, e2101460.